

UNITED STATES DEPARTMENT OF INTERIOR
GEOLOGICAL SURVEY

SCHLUMBERGER SOUNDINGS, AUDIO-MAGNETOTELLURIC SOUNDINGS
AND TELLURIC MAPPING IN AND AROUND THE
COSO RANGE, CALIFORNIA

BY

Dallas B. Jackson, James E. O'Donnell, and Daniel I. Gregory

Open-File Report 77-120

1977

This report is preliminary
and has not been edited or
reviewed for conformity
to Geological Survey standards.

SCHLUMBERGER SOUNDINGS, AUDIO-MAGNETOTELLURIC SOUNDINGS (R. S. Sup. Vol. 2 pp. 360, Sec. 749)

AND TELLURIC MAPPING IN AND AROUND THE
COSO RANGE, CALIFORNIA

by

Dallas B. Jackson, James E. O'Donnell, and Daniel I. Gregory

In 1975 the U.S. Geological Survey began a program of geophysical surveys in and around the Coso Range, and in particular in the area surrounding Coso Hot Springs, to investigate electrical properties of rocks associated with thermal phenomena of the Devil's Kitchen-Coso Hot Springs area in the Coso rhyolite dome field (Duffield and Bacon, 1976) and the large arcuate fracture system (Fig. 1) that Duffield (1975) has postulated may represent a stage of incipient caldera formation.

Figure 1.--NEAR HERE

Plate 1 shows the index map for the location of the 18 U.S. Geological Survey Schlumberger (U.S.G.S) soundings and 6 Schlumberger (HR and C) soundings made by Ferguson (1973). In addition plate 1 also includes the location of audio-magnetotelluric (AMT) cross sections A-A' and B-B' (Plates 2 and 3), and D.C. resistivity cross sections D-D' and C-C' (Plates 4 and 5).

All the U.S. Geological Survey Schlumberger sounding curves were automatically processed and interpreted (Zohdy, 1973 and 1975) as shown in the graphs given in appendix I.

Each graph shows the following:

- (1) Field data designated by a solid line curve with diamond symbols

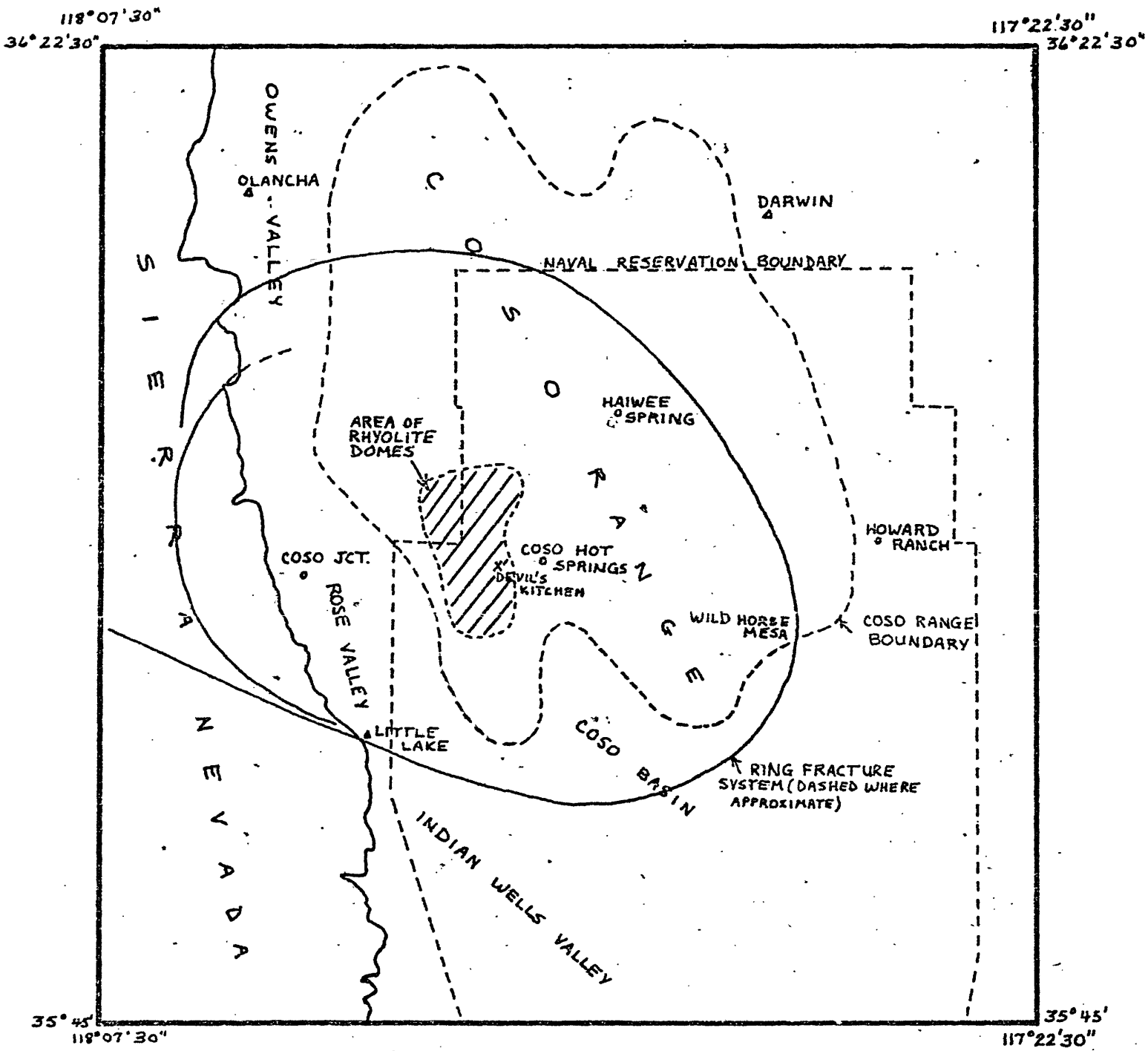


Figure 1.--General location map of the Coso Range and surrounding area.

for observed data.

(2) A dashed curve which represents:

- (a) The continuous or shifted "field" curve which usually is obtained by maintaining the position of the last segment and shifting each of the previous segments, up or down so that the last point on each segment coincides with the corresponding point on the following segment (Zohdy and others, 1973).
 - (b) The digitized curve at the sampling interval of 6 points per logarithmic cycle. Although the individual digitized points are not depicted on the dashed curve (to avoid cluttering the graphs) they were computed using a subroutine in a computer program for bicubic spline functions (Anderson, 1971). The digitized data from the dashed curve were then fed into the automatic interpretation program (Zohdy, 1973) to obtain the best fitting theoretical sounding curve for a horizontally layered medium. The automatic interpretation program used here was slightly modified from the one referred to in the above reference. The modifications are identical to those used in another program recently written for inverting Wenner sounding curves (Zohdy and Bisdorf, 1975).
- (3) The theoretical best fitting sounding curve plotted as (+) signs.
 - (4) The detailed layering for which the theoretical curve is calculated.
 - (5) The D.Z. (Dar Zarrouk) curve (plotted as dots) for the detailed

layering. The ordinates values for the D.Z. curves are shifted upward or downward by one logarithmic cycle to avoid cluttering the graphs, or they are plotted on a separate sheet of graph paper (as for example USGS 3 and 5).

The D.Z. curves can be used to obtain equivalent and simpler solutions containing fewer numbers of layers. Also they can be used to impose certain constraints on the layer thicknesses and resistivities (Zohdy, 1974). The above technique was used to modify the detailed solutions from the automatic interpretations for the D.C. soundings shown on cross sections B-B' and C-C' (Plates 4 and 5). The layering shown on the 2 cross sections and the theoretical curves calculated from the layering (i.e. the forward solutions) compared to their respective shifted field curves ^{1/}are shown on the graphs in appendix II for the U.S. Geological Survey soundings. No attempt was made to shift field curve segments on soundings HR-2, HR-5, HR-6, HR-9, HR-10, or C-3. The theoretical curves for these soundings are plotted directly over the Schlumberger field points as they appear in Furgerson, pages 42-52 (1973). The field points on the shifted curve on graphs in appendix II are represented by circles and for the theoretically calculated curve are represented by triangles. On sounding curves U.S.G.S. 4, 6, and HR-9 in appendix II a half space of infinite resistivity has been added beneath the last layer interpreted from the field data to estimate an approximate minimum depth to a high resistivity basement. ^{2/}

^{1/}The shifted field curves correspond to the dashed curves in appendix I.

^{2/}As the resistivity of the basement halfspace decreases so will the depth to its top.

The AMT soundings used natural electromagnetic fields at 10 frequencies from 7.5 HZ to 6.7 KHz and an artificial field broadcast from VLF radio stations operating at 10.2 and 18.6 KHz. All the soundings were made using a two channel scalar instrument. After measuring impedances in an x direction, the coil and E line were rotated 90^o, to measure impedances in the a y direction. To prepare skin depth pseudo-sections, the log average of impedances in both directions were used (Hoover and Long, 1975). The skin depth in meters, δ , at which each resistivity was plotted and then contoured on the depth pseudo-sections was calculated from

$$\delta = 503 \sqrt{\rho_a t}$$

where ρ_a is apparent resistivity in ohm-meters and t is period in seconds.

The telluric current data was recorded using a band width from 10 to 60 seconds with most of the energy being present about the 20 second range, and recorded by the x-y plotter method of Yungul (1966). K values were calculated by taking a ratio of ellipse areas of the rover station to the base station (Yungul, 1968) and these contoured at a logarithmic interval (plate 6). The base station for the telluric survey, about 2 km west of Coso Hot Springs (plate 6), was assigned a K value of 10. Contours of K less than 10 imply lower resistivity values than at the base station.

The telluric map, plate 6, shows the major resistivity features of the survey area. The basic pattern is a low over Rose Valley, a moderate high over the eastern Coso Range, a low over the Coso Basin that possibly extends northward into the alluvial valley east of Coso Hot Springs and a general high over the western Coso Range that includes the rhyolite dome field. The low resistivity areas over Rose Valley (a southern extension of Owen's Valley) and the Coso Basin are probably related to conductive

valley fill; possibly a combination of fine grained sedimentary rocks and saline ground water.

The west end of cross section D-D' (Plate 5) shows the conductive nature and depth of the geologic section near Coso Junction and is in rough agreement with interpretations of the same area by Fugerson, 1973 and Healy and Press, 1964. At U.S.G.S. sounding 14 the basement appears to be resistive (see also appendix II), but there are no heat flow measurements to indicate whether or not the valley might contain hot waters.

The resistivity low over the Coso Basin is probably related solely to conductive valley fill as shown on cross section C-C' (Plate 4) at sounding U.S.G.S. 11. A heat flow value of 2.4 HFU (Plate 6) less than 2 km to the SSW of sounding U.S.G.S. 11 at the edge of the basin suggests that the cause of the low resistivity in the basin is not related to a heat source.

The source of the low resistivity zone to the north of Coso Basin in the area around Coso Hot Springs is clear from the D.C. cross section D-D' (plate 5). In and to the west of the Devil's Kitchen area (an area of very high heat flow) a low resistivity horizon ranging from about 5 to 10 ohm-m and about 300 m thick overlies a high resistivity zone of indeterminate thickness. The effect of the low resistivity horizon is also apparent on the AMT cross sections at sounding 2, plates 2 and 3. Since most rocks of the highly fractured Sierran basement complex in the western Coso Range have resistivities of only about 150-250 ohm-m, it seems probable that the near surface low resistivity layer mentioned above is a highly altered-impervious layer capping a high resistivity

vapor dominated thermal system in the fractured basement rocks. Based on heat flow and microearthquake data Combs and Rotstein also postulate a vapor dominated system underlying part of the rhyolite dome field (Combs, 1975; Combs and Rotstein, 1976). Slightly further west at sounding U.S.G.S. 16 (plate 5) the basement rocks have a resistivity of 95 ohm-m or less and probably contain hot waters. As far as 5 km east of Coso Hot Springs, under the main part of the telluric K value low, the resistivity soundings suggest that there is a section of material up to 1800 m thick having resistivities as low as 5 ohm-m. This wedge of low resistivity material may be an eastward dipping structural basin filled with a combination of alluvial debris and flows; it may also be a zone of very intense fracturing of the basement rocks containing hot waters, or most likely a combination of both. The geologic map by Duffield and Bacon shows this to be a zone of numerous N to NW oriented faults. Two heat flow holes with ⁱⁿ the K value low east of Coso Hot Springs, plate 6, have values of 3.7 and 4.4 HFU. Both of these values are above the regional average for the Basin and Range Province and probably reflect hot water runoff from the probable steam zone to the west collecting in the structural low.

As mentioned previously, the rhyolite dome field and the Coso Range north of the dome field is a resistivity high compared to the surrounding valleys. The general trend of relatively high telluric K values over this area is not surprising when one considers that the larger part of the rocks, even where they may contain hot waters such as sounding U.S.G.S. 16, are composed of Sierran basement complex with a thin veneer of volcanics and have resistivities probably greater than 50 ohm-m. Locally around the

fumerolic areas the K values are some what, but not dramatically lower. Certainly over a vapor dominated system or even a hot water system in fractured igneous rocks a relatively high resistivity environment might be expected when compared with adjacent deep sedimentary basins.

AMT cross sections A-A' and B-B', Plates 2 and 3, agree qualitatively with the relative highs and lows on the telluric K value map and the interpreted D.C. resistivity sections, where they parallel each other. The only place on the dome field that the AMT soundings identify a low resistivity section is at AMT station 6.^{1/} This corresponds to the low resistivity layer between soundings U.S.G.S. 18 and HR-10 on cross section D-D' and suggests the cap rock for the vapor dominated system does not go as far north as AMT station 3 or as far east as AMT station 7.

If our assumptions about the electrical properties of a vapor dominated system around Devil's Kitchen are correct then a network of the AMT stations might define the lateral extent of the low resistivity layer (cap rock?). Additional Schlumberger soundings may also be useful, although the rugged terrain within the dome field severely limits their placement and length of expansion.

^{1/}The low at AMT station 6 reflects a combination of the eastern edge of the conductive zone seen at HR-10 and low resistivity zone at the west edge of the dome field in the valley fill.

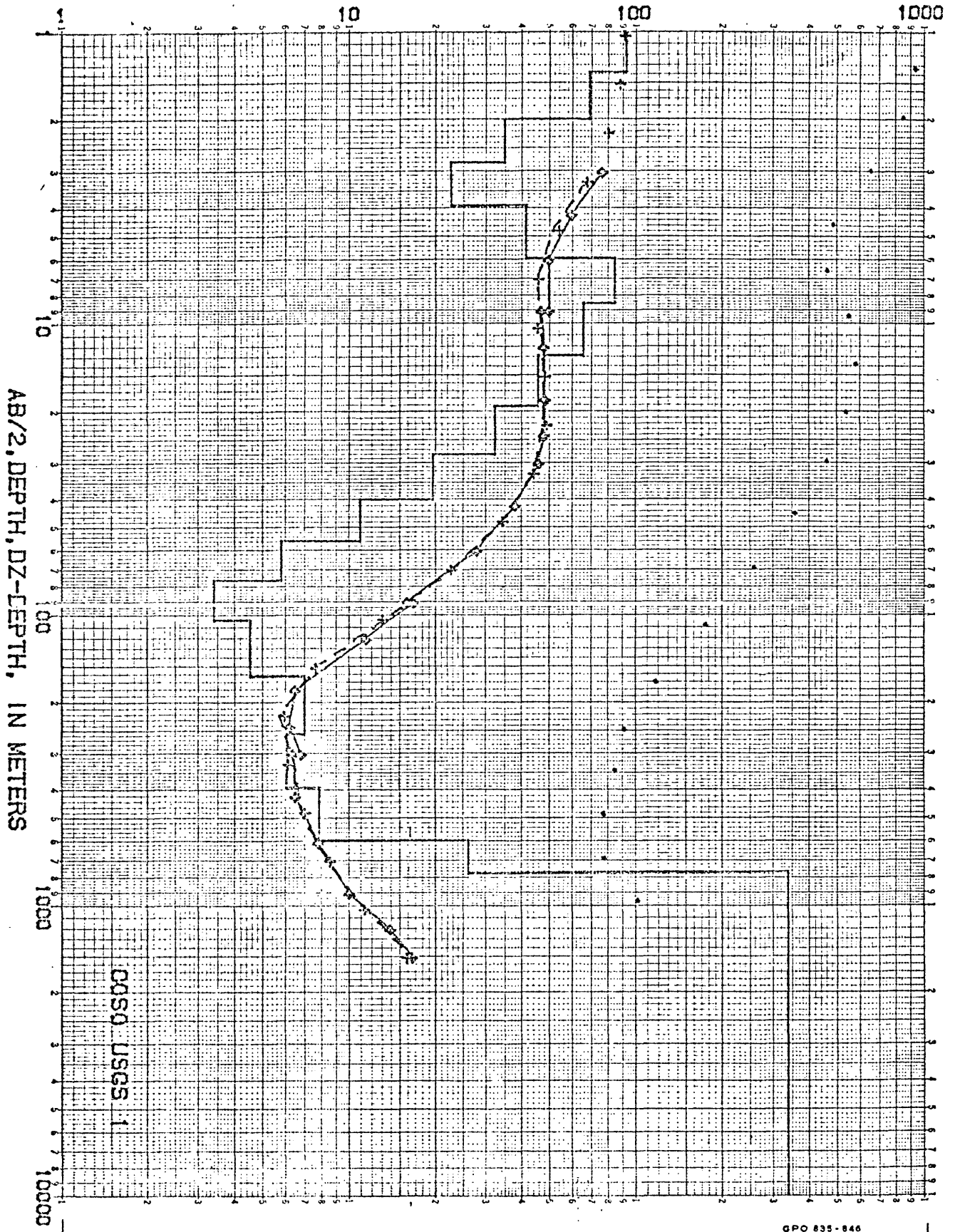
REFERENCES

- Anderson, W. L., 1971, Application of bicubic spline functions to two dimensional grided data: NTIS (National Technical Information Service), No. PB-203579, Springfield, Virginia.
- Combs, J., 1975, Heat flow and microearthquake studies, Coso Geothermal Area, China Lake, California: Final report to Advanced Research Projects Agency, ARPA Order No. 2800, Contract No. N00123-74-C-2099, 65 pp.
- Combs, J., and Rotstein, Y., 1976, Microearthquake studies at the Coso Geothermal Area, in Proceedings of Second United Nations Symposium on the Development and Use of Geothermal Resources, in press.
- Duffield, W. A., 1975, Late Cenozoic ring faulting and volcanism in the Coso Range of California, Geology, v. 3, p. 335-338.
- Duffield, W. A., and Bacon, R., 1976, Preliminary geologic map of the rhyolite domes and adjacent area, Inyo County, California, U.S. Geol. Survey Open-File Report 76-238.
- Furgerson, R. B., 1973, Progress report on electrical resistivity studies, Coso geothermal area, Inyo County, California: Naval Weapons Center Tech. Pub. 5497, 38 pp.
- Healy, J. H., and Press, Frank, 1964, Geophysical studies of basin structures along the eastern front of the Sierra Nevada, California: Geophysics, v. 24, no. 3, p. 337-359.
- Hoover, D. B., and Long, C. L., 1975, Audio-magnetotelluric methods in reconnaissance geothermal exploration: U.S. Geol. Survey Open-File Rept. 75-362.

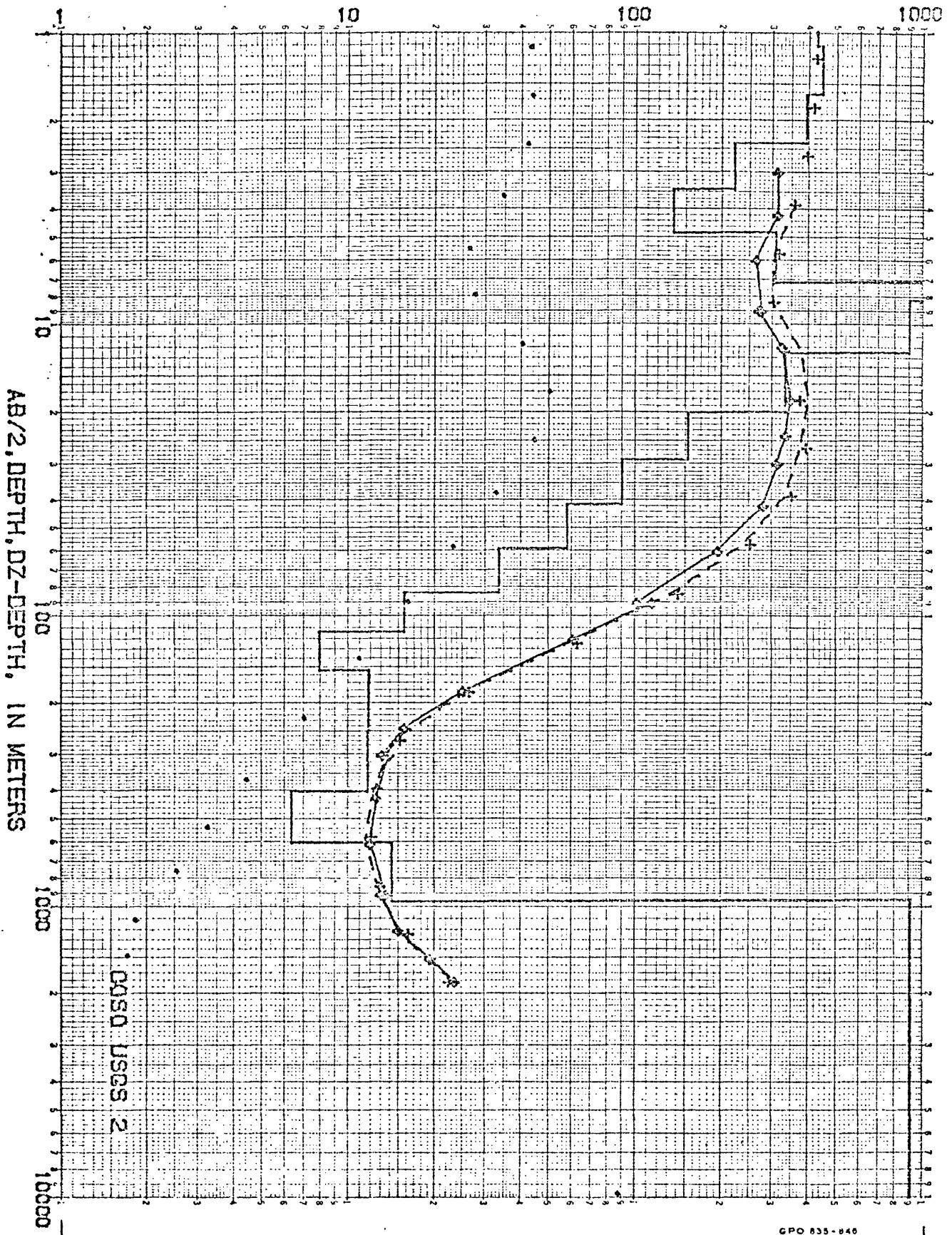
- Yungül, S. H., 1966, A magnetotelluric method without magnetic measurements: Geophysics, v. 31, no. 1, p. 185-191.
- _____, 1968, Measurements of telluric relative ellipse area by means of vectograms: Geophysics, v. 33, no. 1, p. 127-131.
- Zohdy, Adel A. R., 1973, A computer program for the automatic interpretation of Schlumberger sounding curves over horizontally stratified media: NTIS (Natl. Tech. Inf. Service) PB-232703/AS, 25 p., Springfield, Virginia.
- _____, 1974, The use of Dar-Zarrouk curves in the interpretation of VES data: U.S. Geol. Survey Bull. 1313-D, 41 p.
- _____, 1975, Automatic interpretation of Schlumberger sounding curves using modified Dar-Zarrouk functions: U.S. Geol. Survey Bull. 1313-E, 39 p.
- Zohdy, A. A. R., Anderson, L. A., and Muffler, L. J. P., 1973, Resistivity self potential, and induced polarization surveys of a vapor-dominated geothermal system: Geophysics, v. 38, p. 1130-1144.
- Zohdy, A. A. R., Bisdorf, R. J., 1975, Computer programs for the forward calculation and automatic inversion of Wenner sounding curves: NTIS (Natl. Tech. Inf. Service) PB-247265/AS, Springfield, Virginia.

APPENDIX I

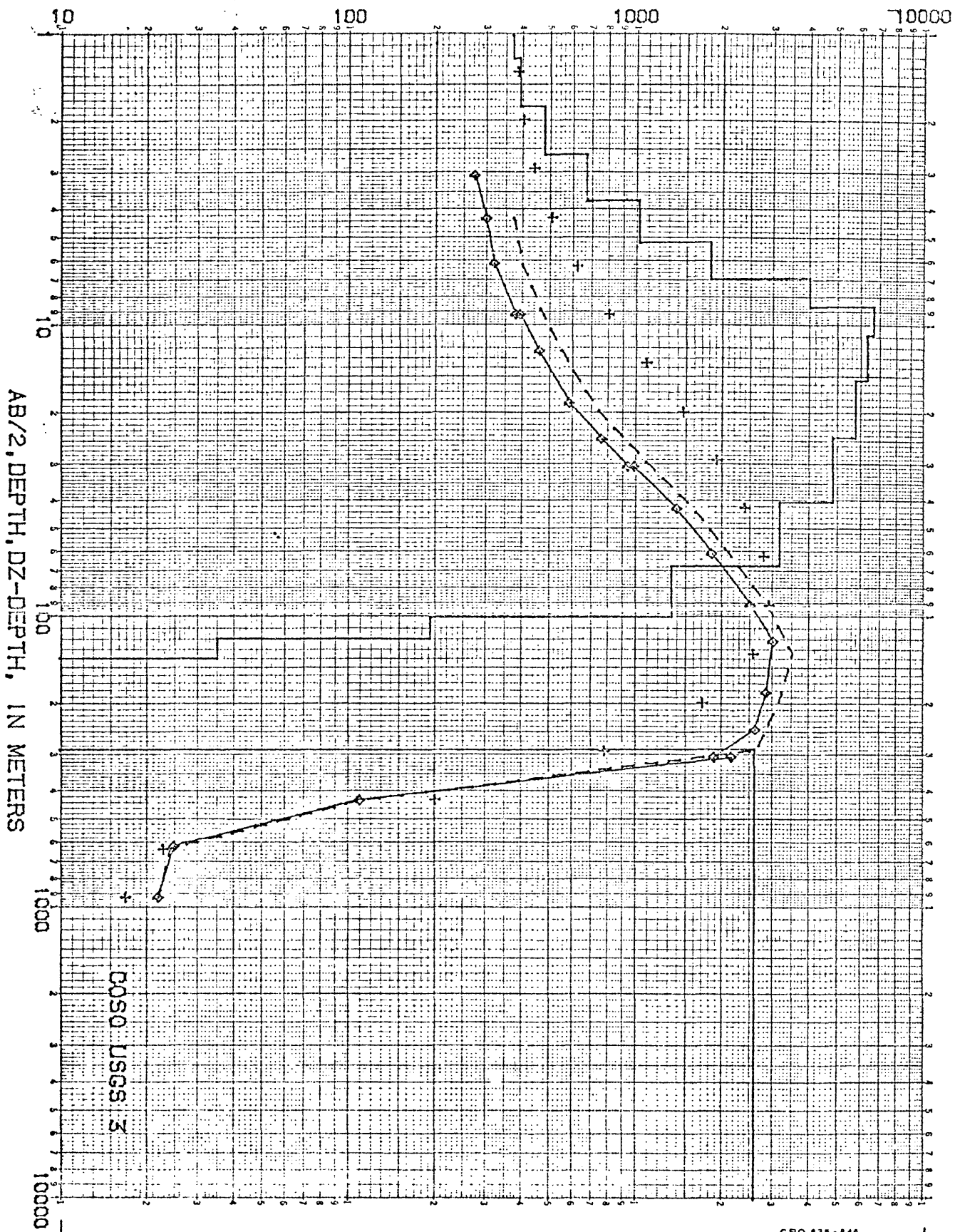
RESISTIVITIES IN OHM-METERS



RESISTIVITIES IN OHM-METERS

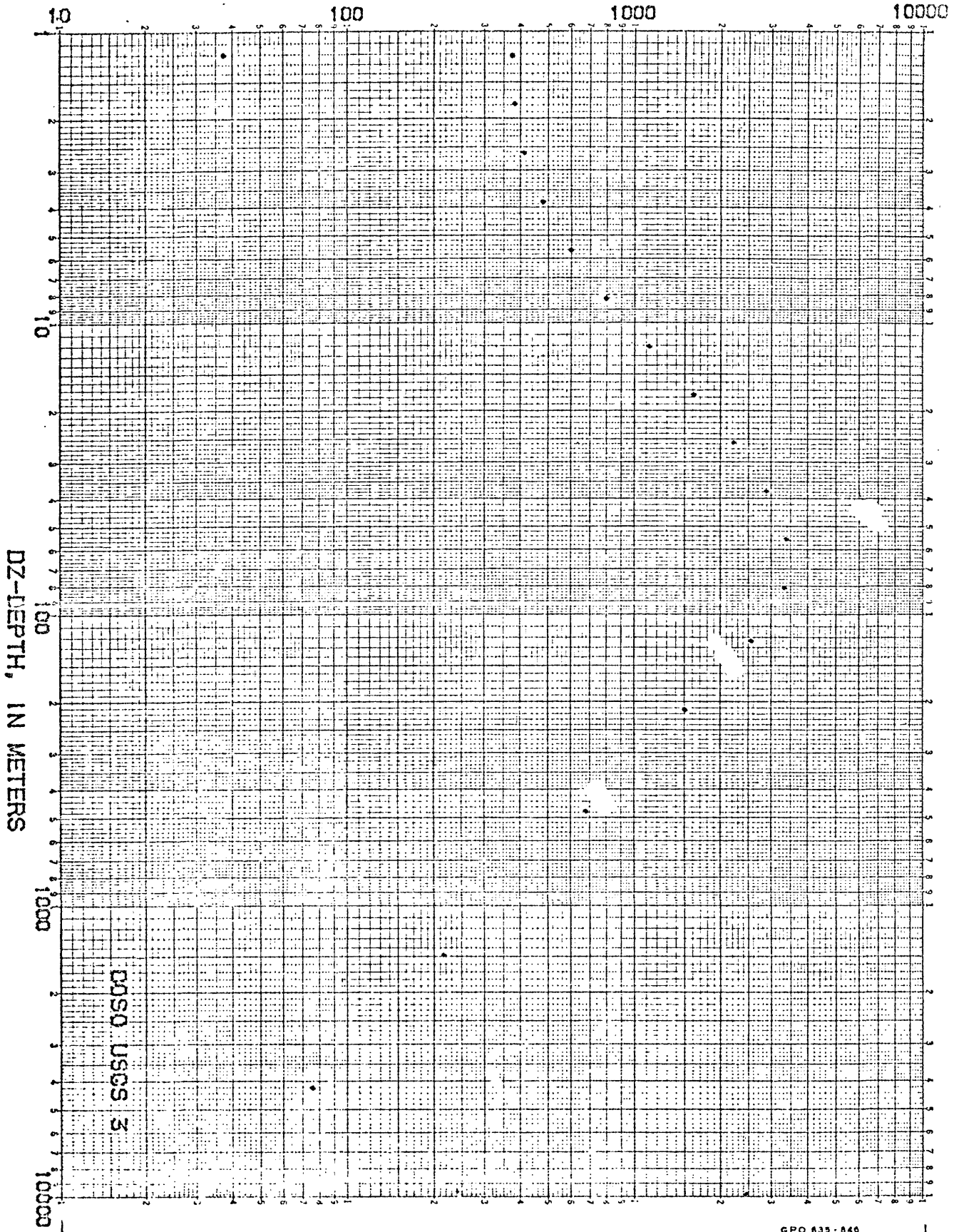


RESISTIVITIES IN OHM-METERS

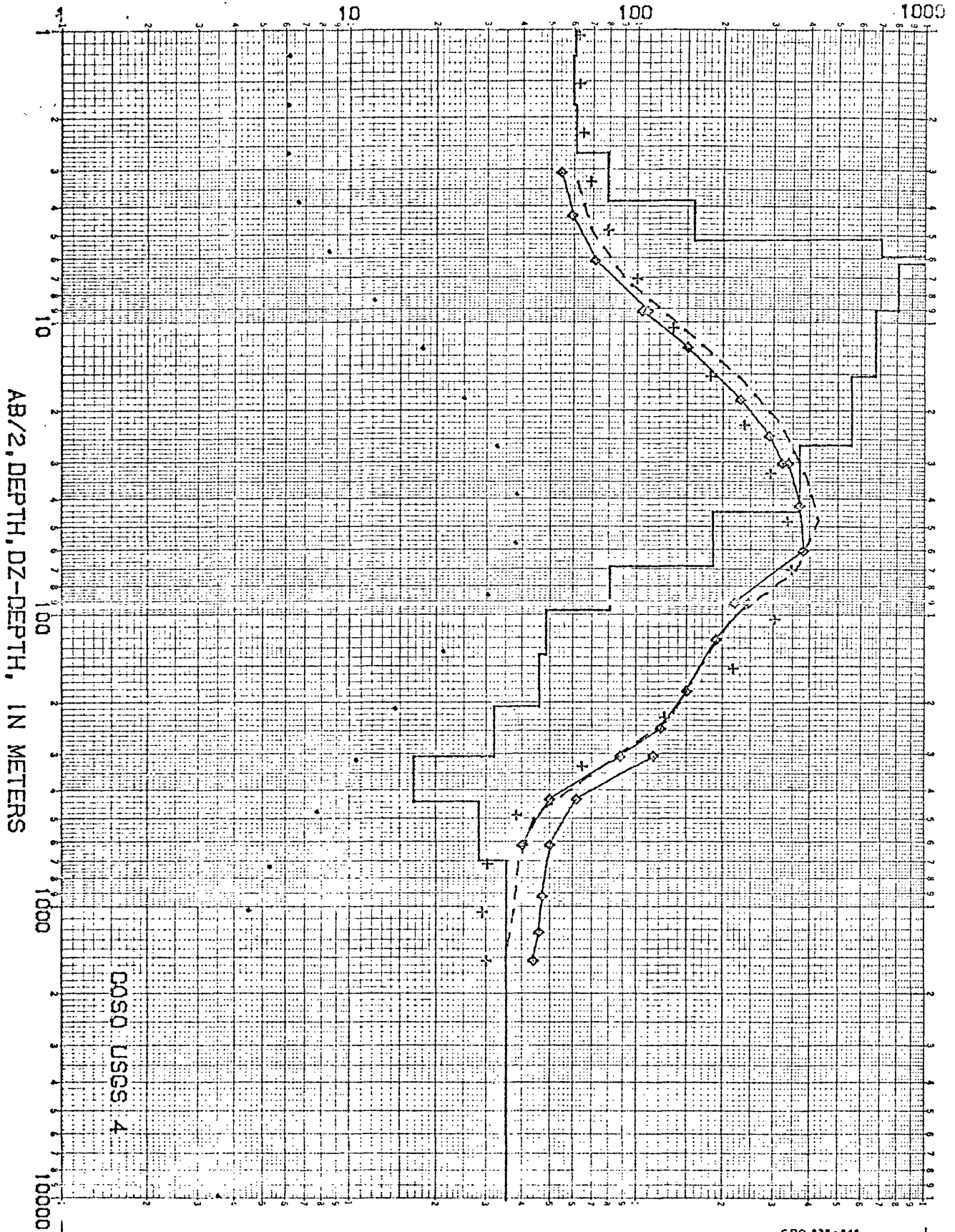


GPO 635-846

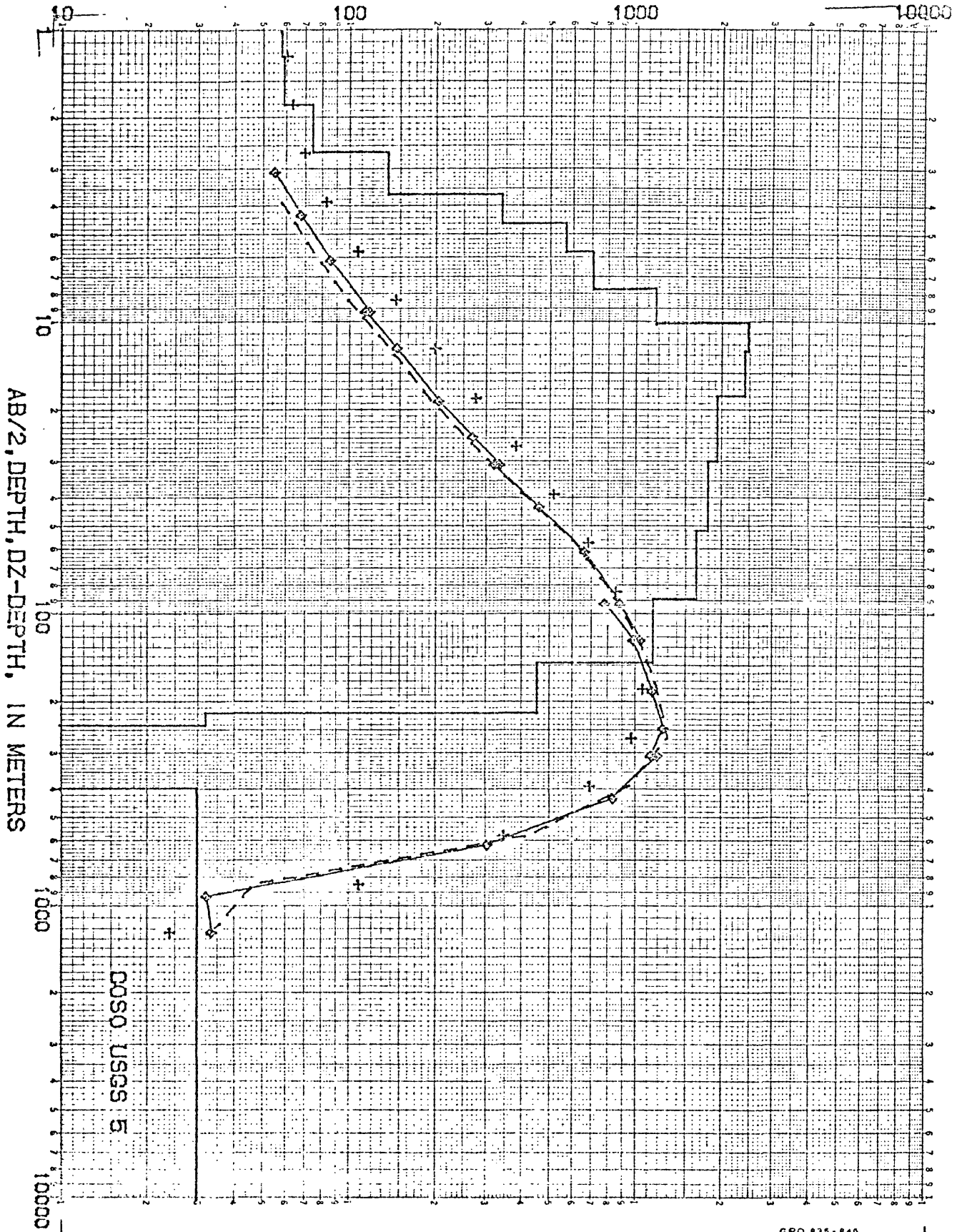
RESISTIVITIES IN OHM-METERS



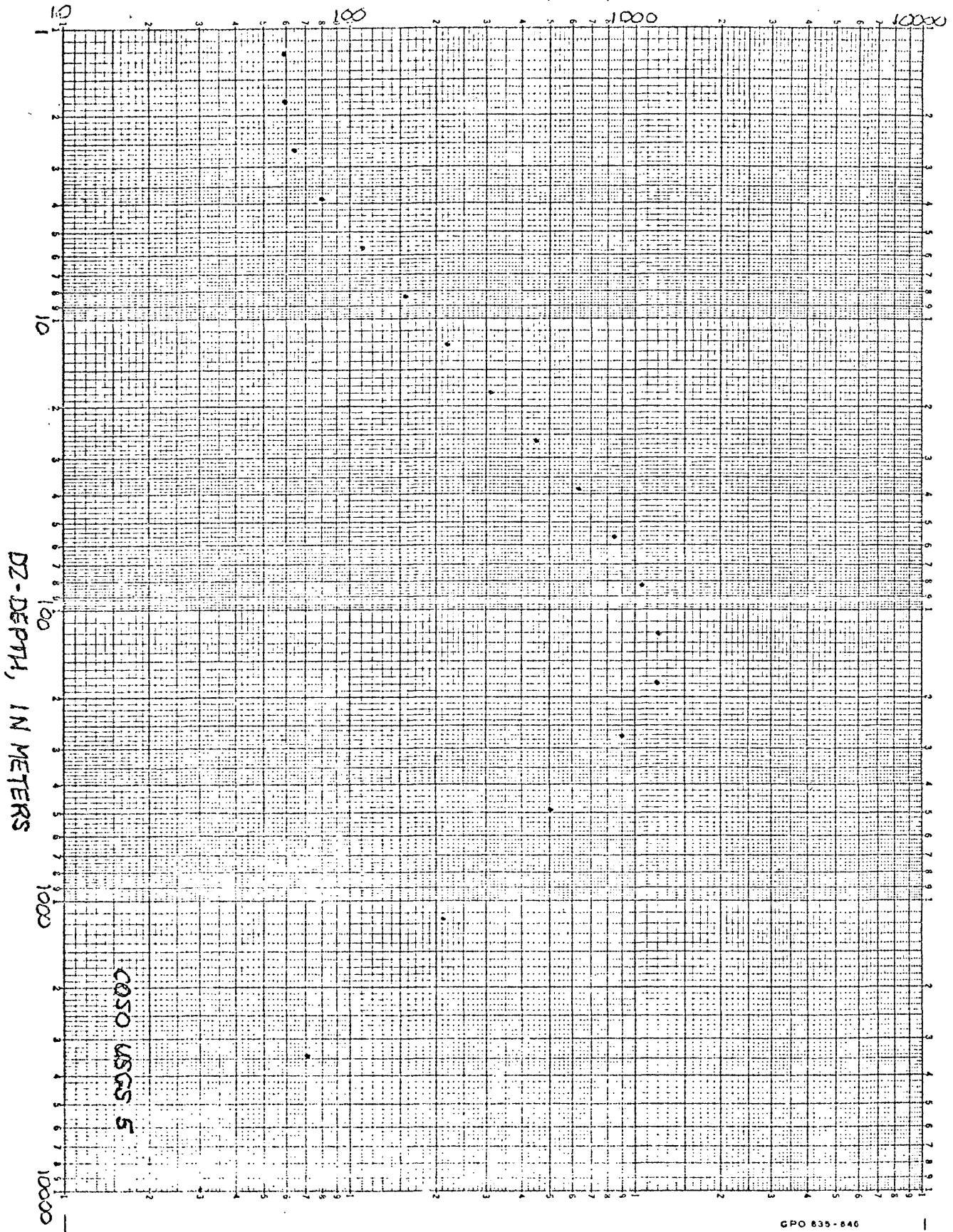
RESISTIVITIES IN OHM-METERS



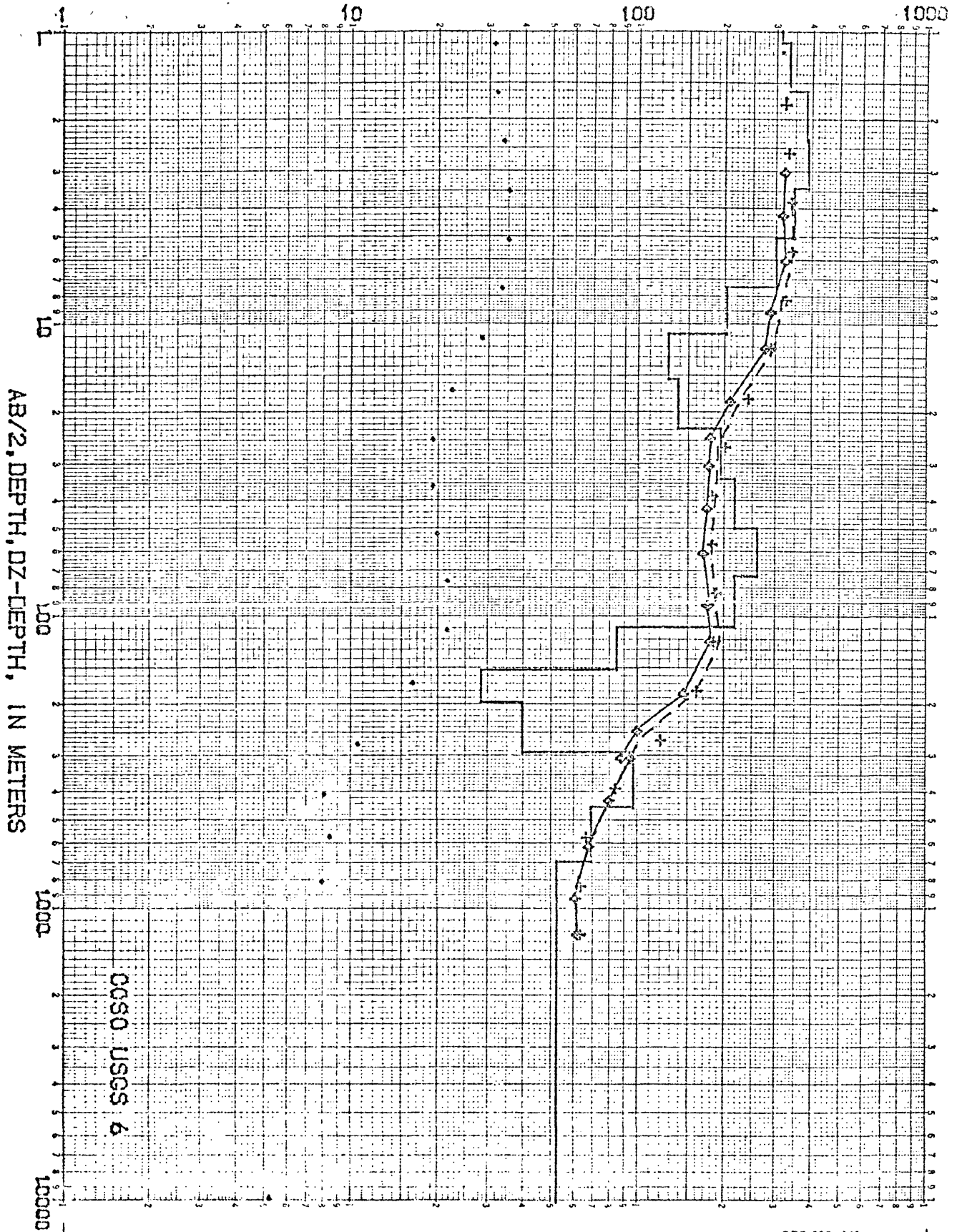
RESISTIVITIES IN OHM-METERS



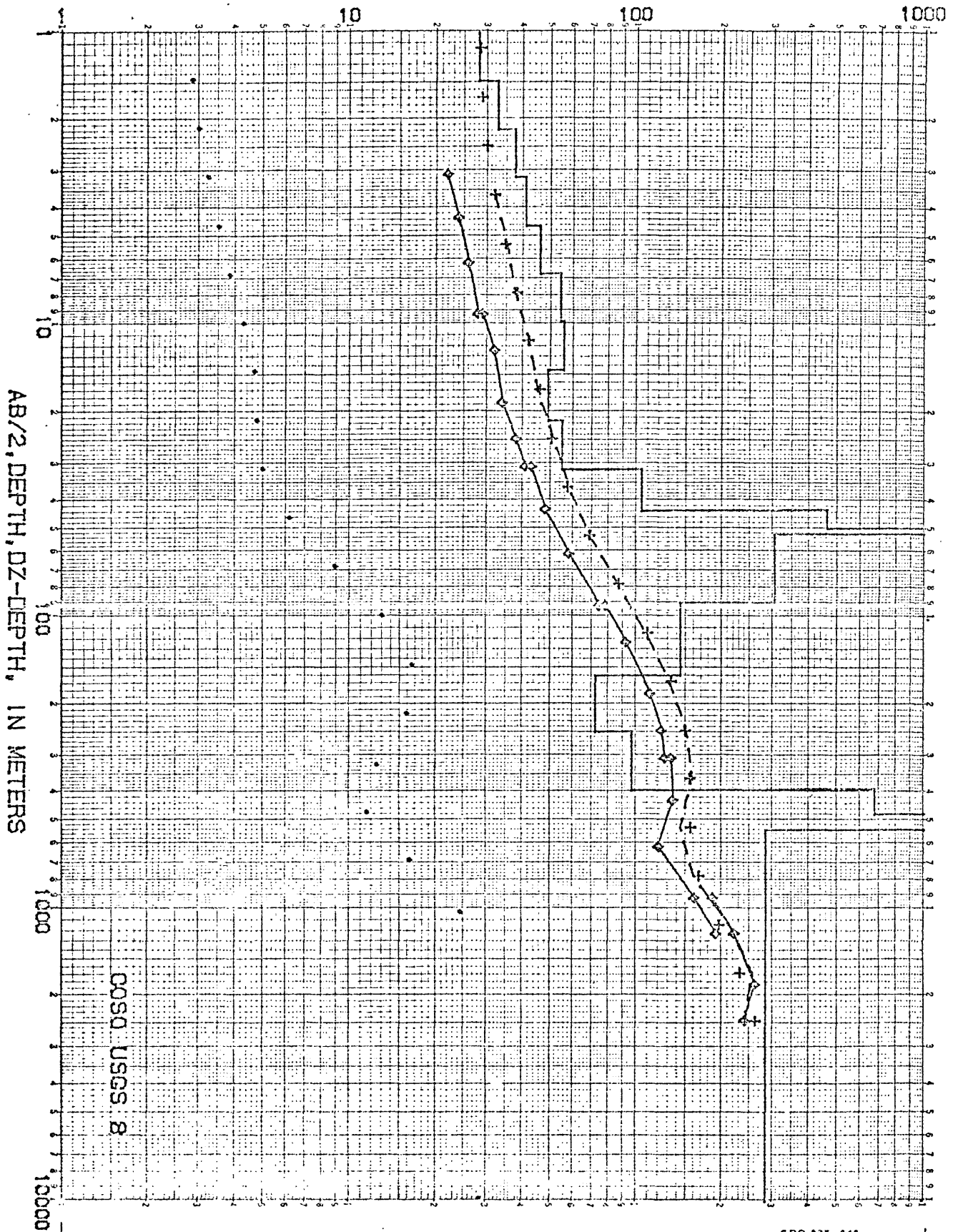
RESISTIVITIES IN OHM-METERS



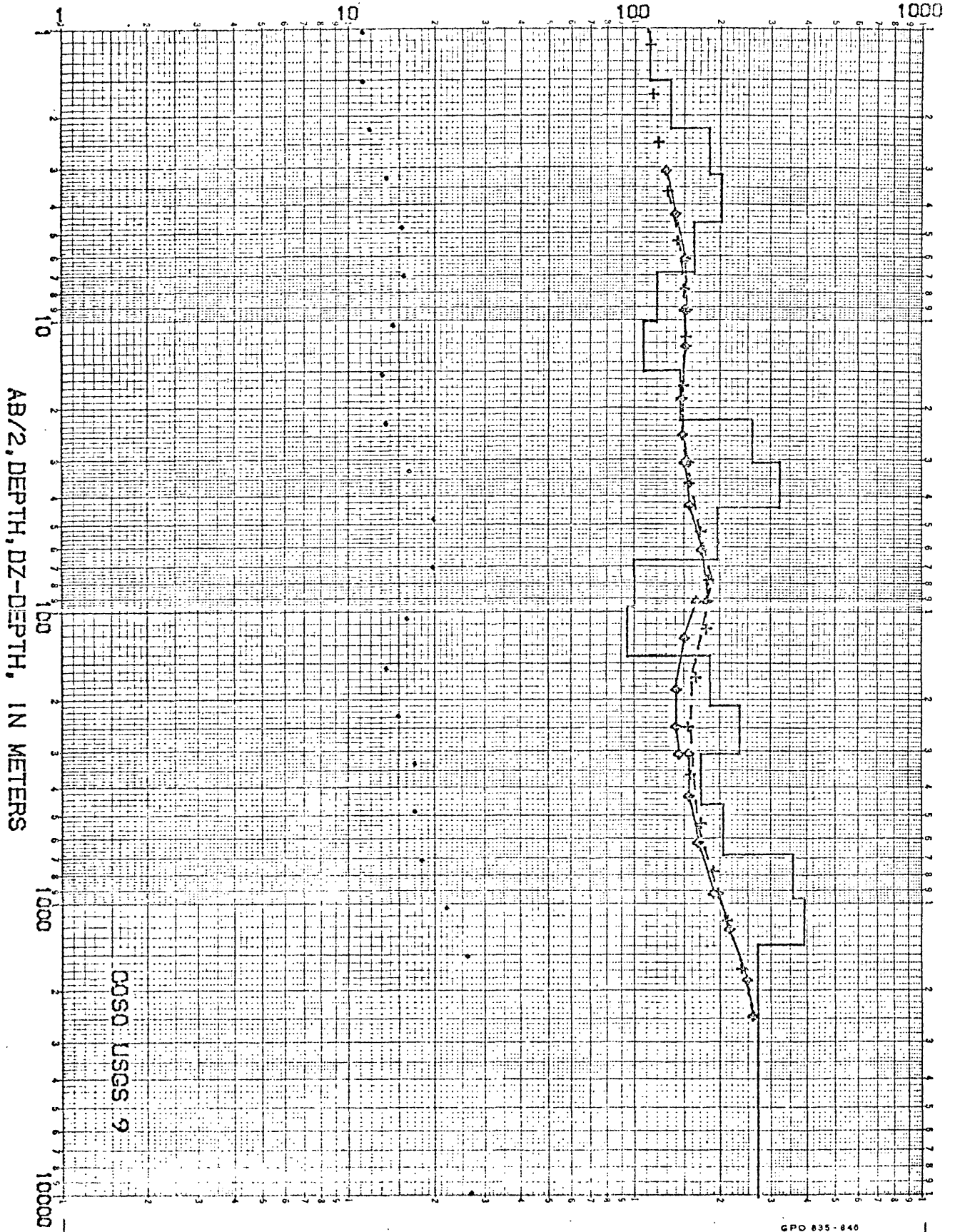
RESISTIVITIES IN OHM-METERS



RESISTIVITIES IN OHM-METERS

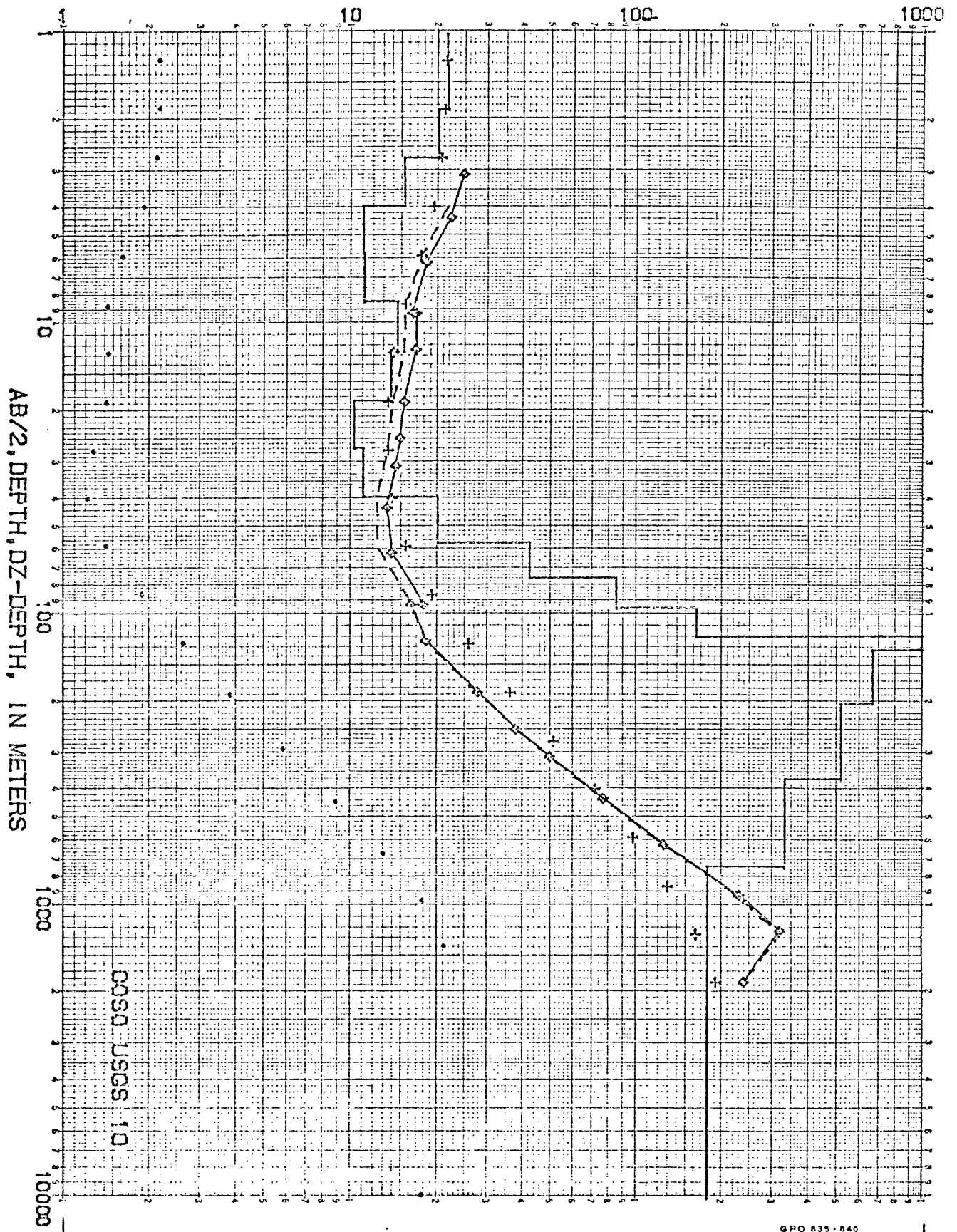


RESISTIVITIES IN OHM-METERS

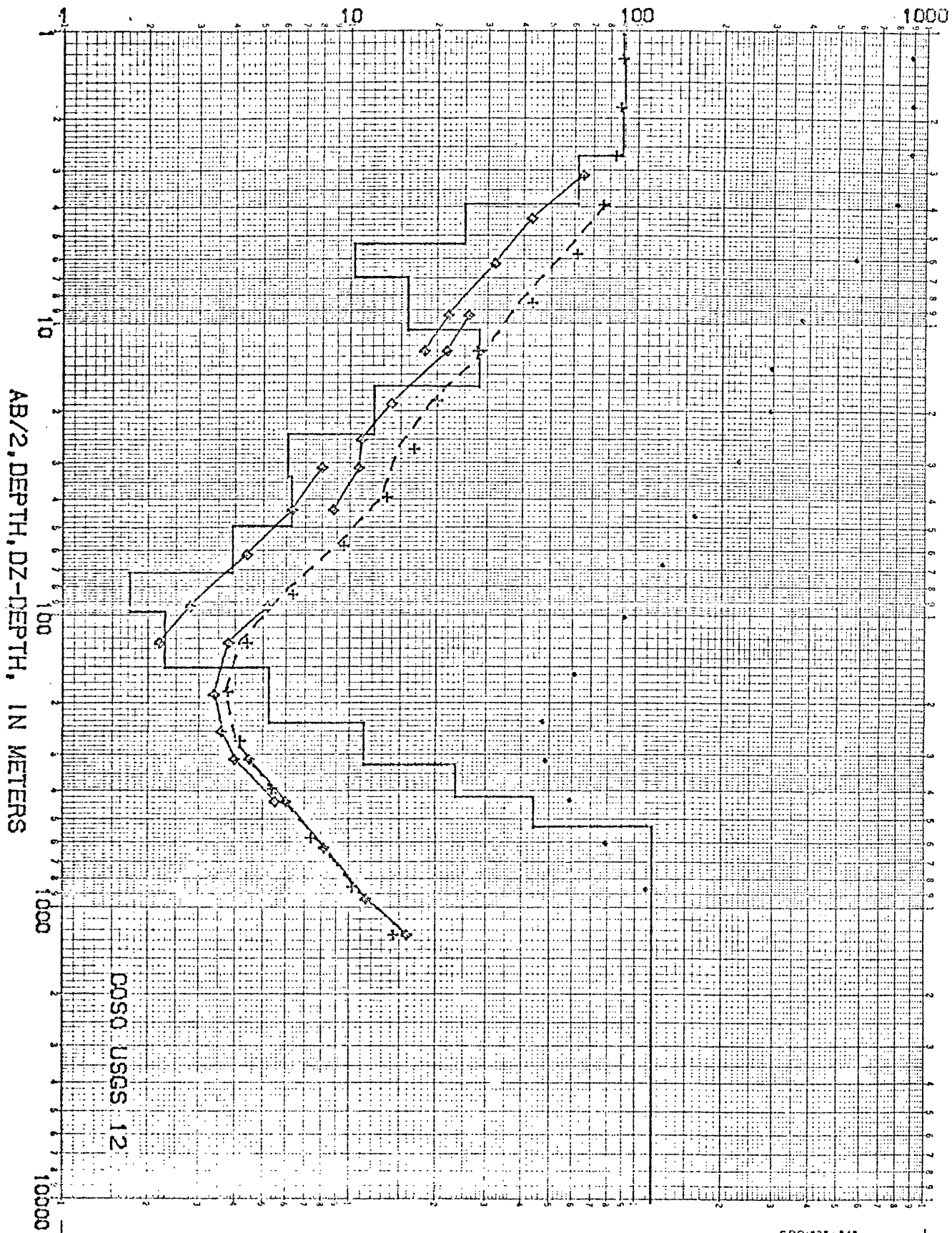


GPO 835-846

RESISTIVITIES IN OHM-METERS

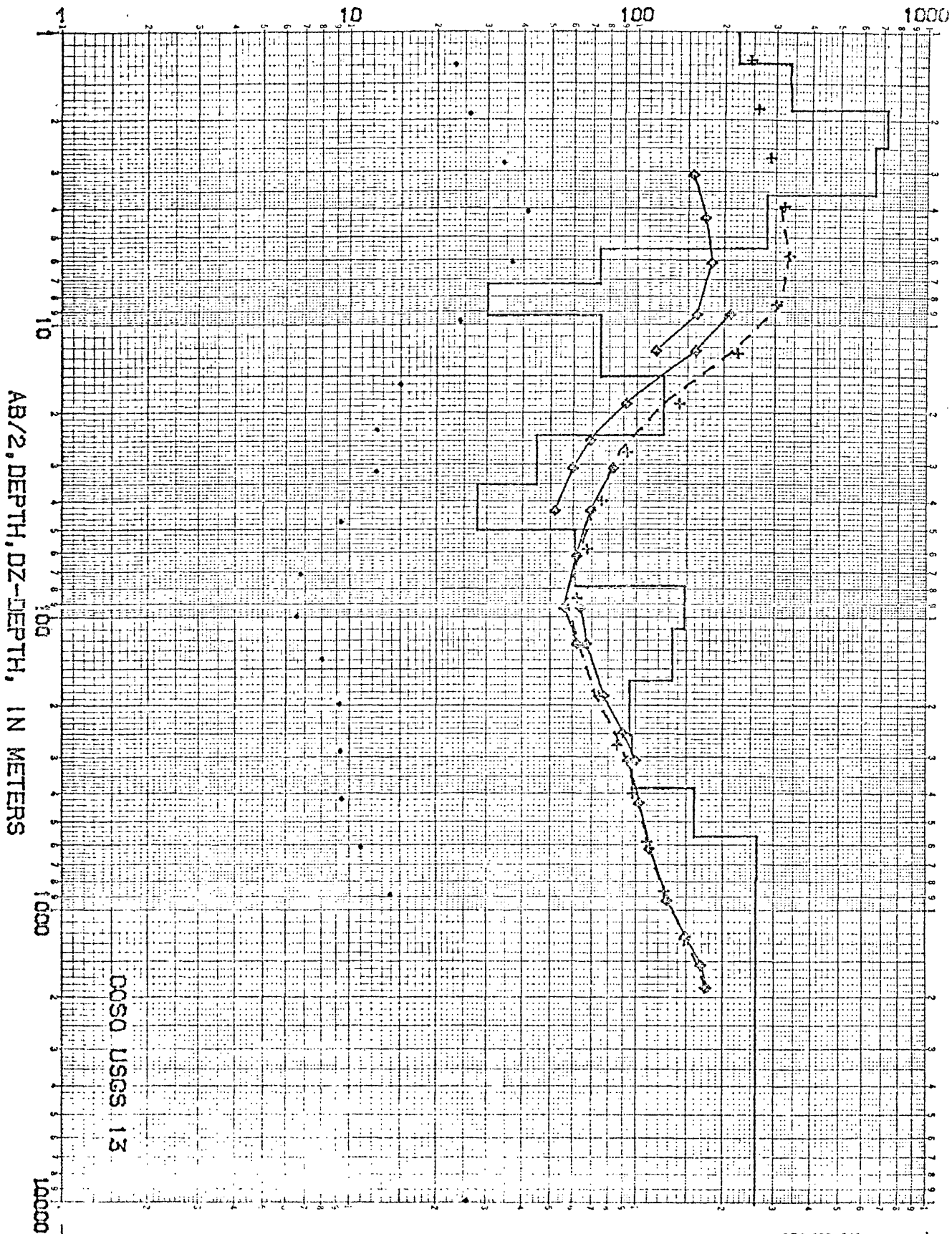


RESISTIVITIES IN OHM-METERS

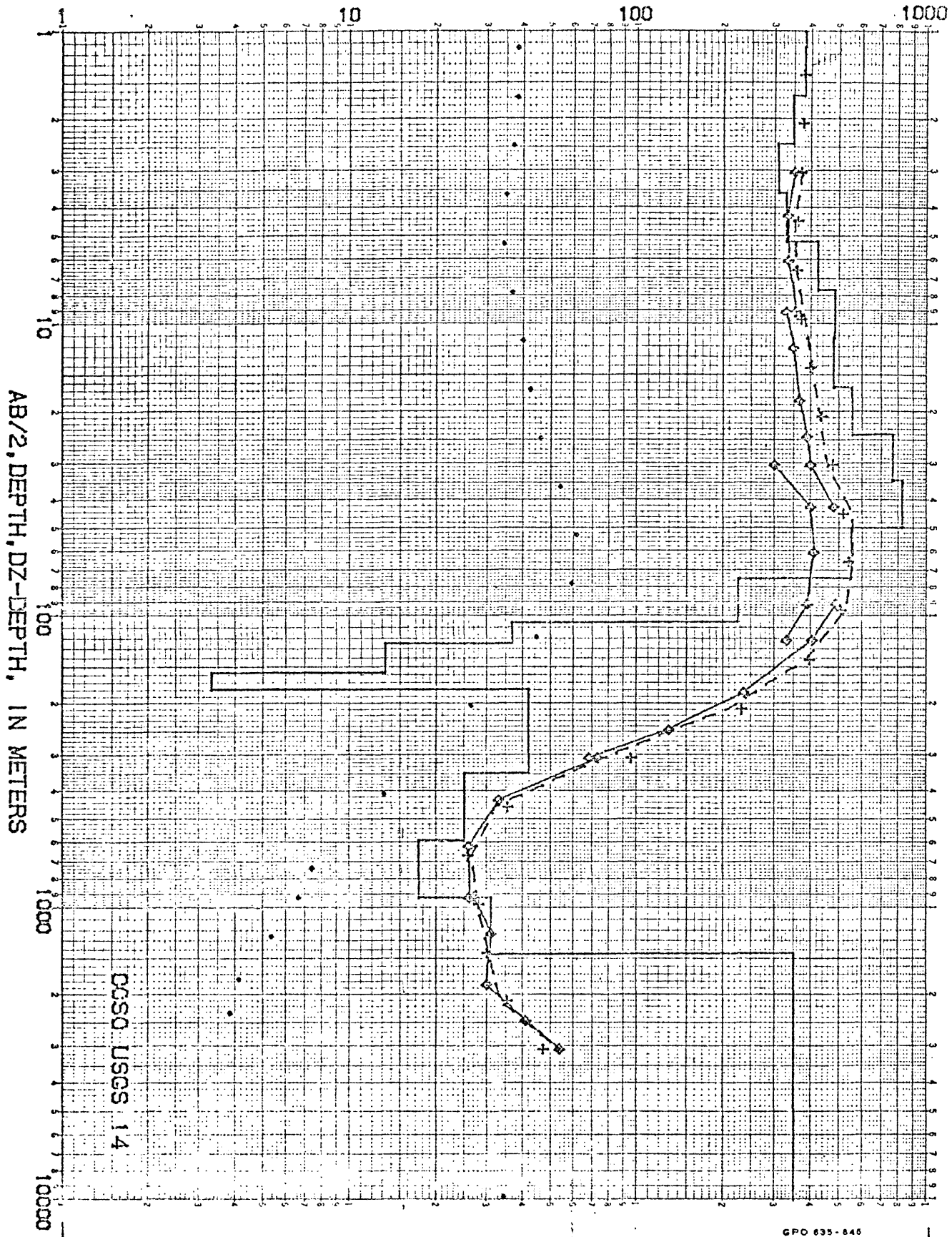


DOSO USGS 12

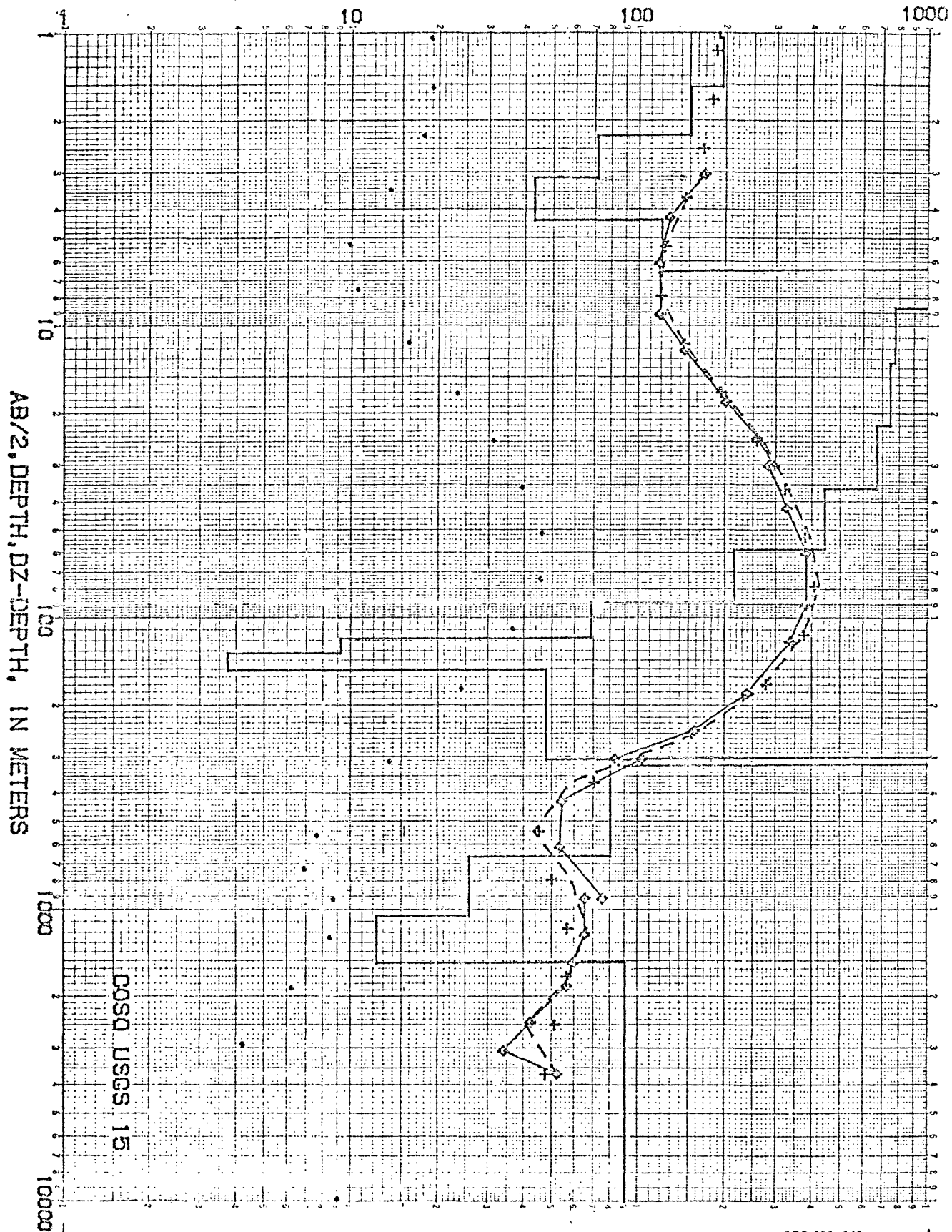
RESISTIVITIES IN OHM-METERS



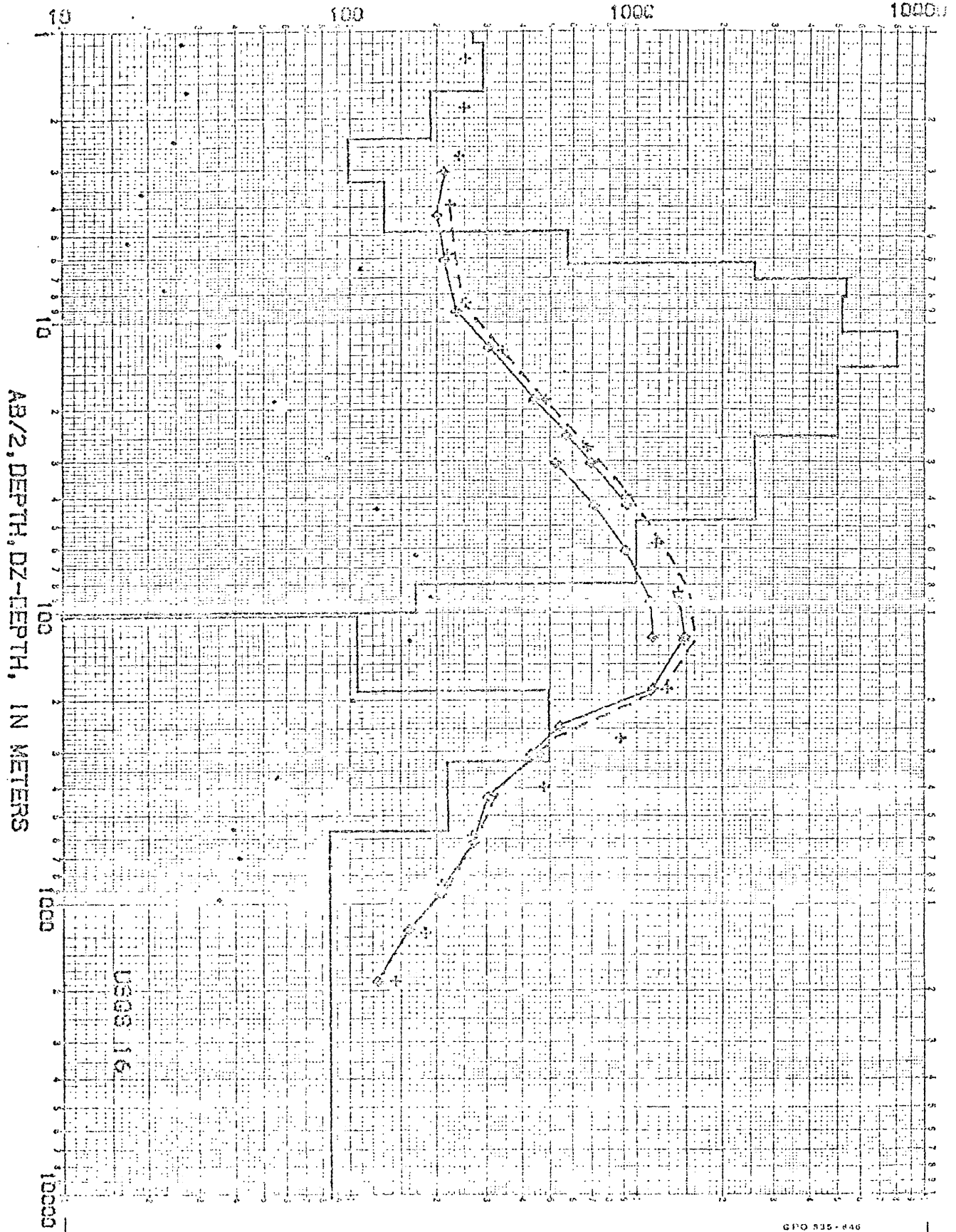
RESISTIVITIES IN OHM-METERS



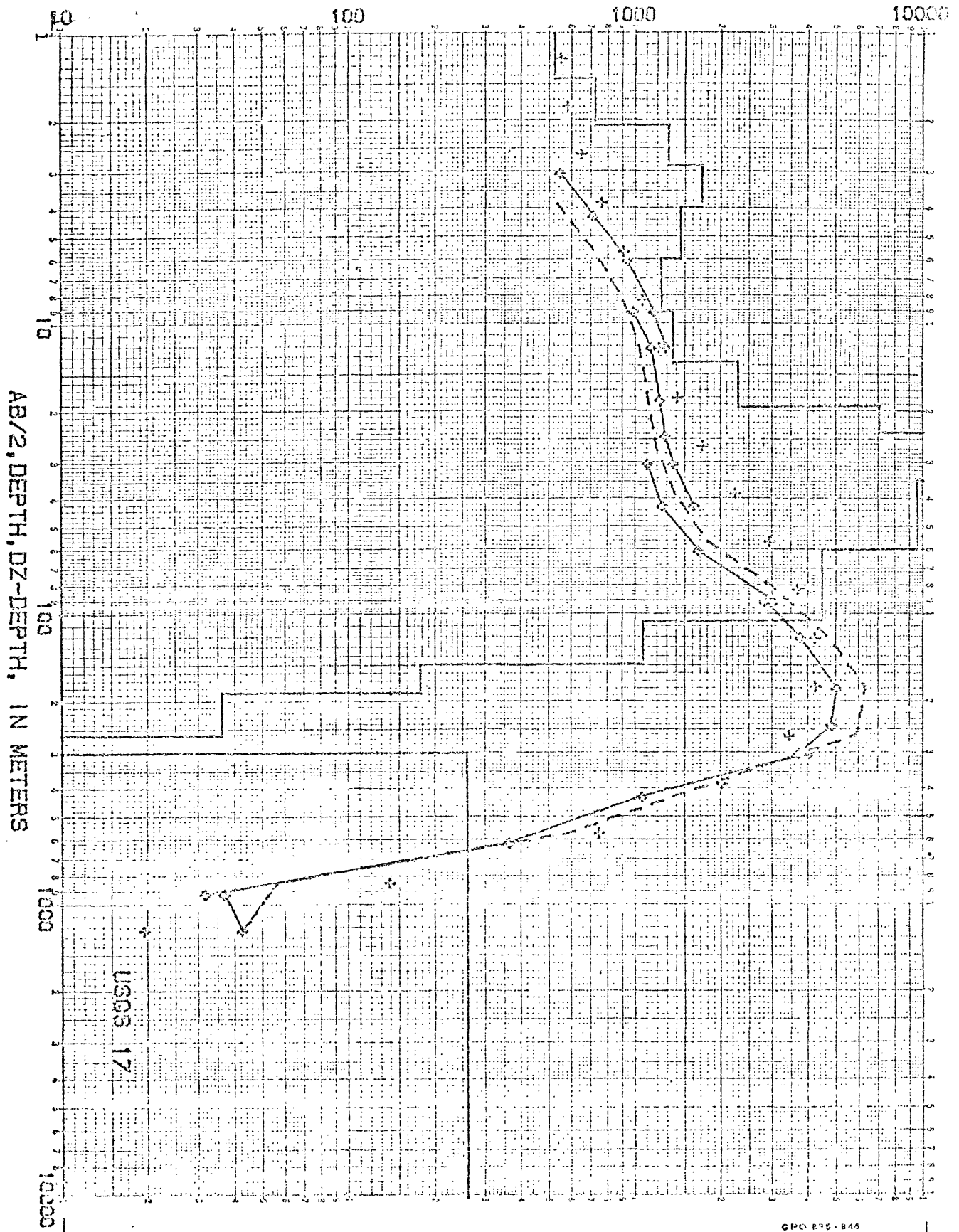
RESISTIVITIES IN OHM-METERS



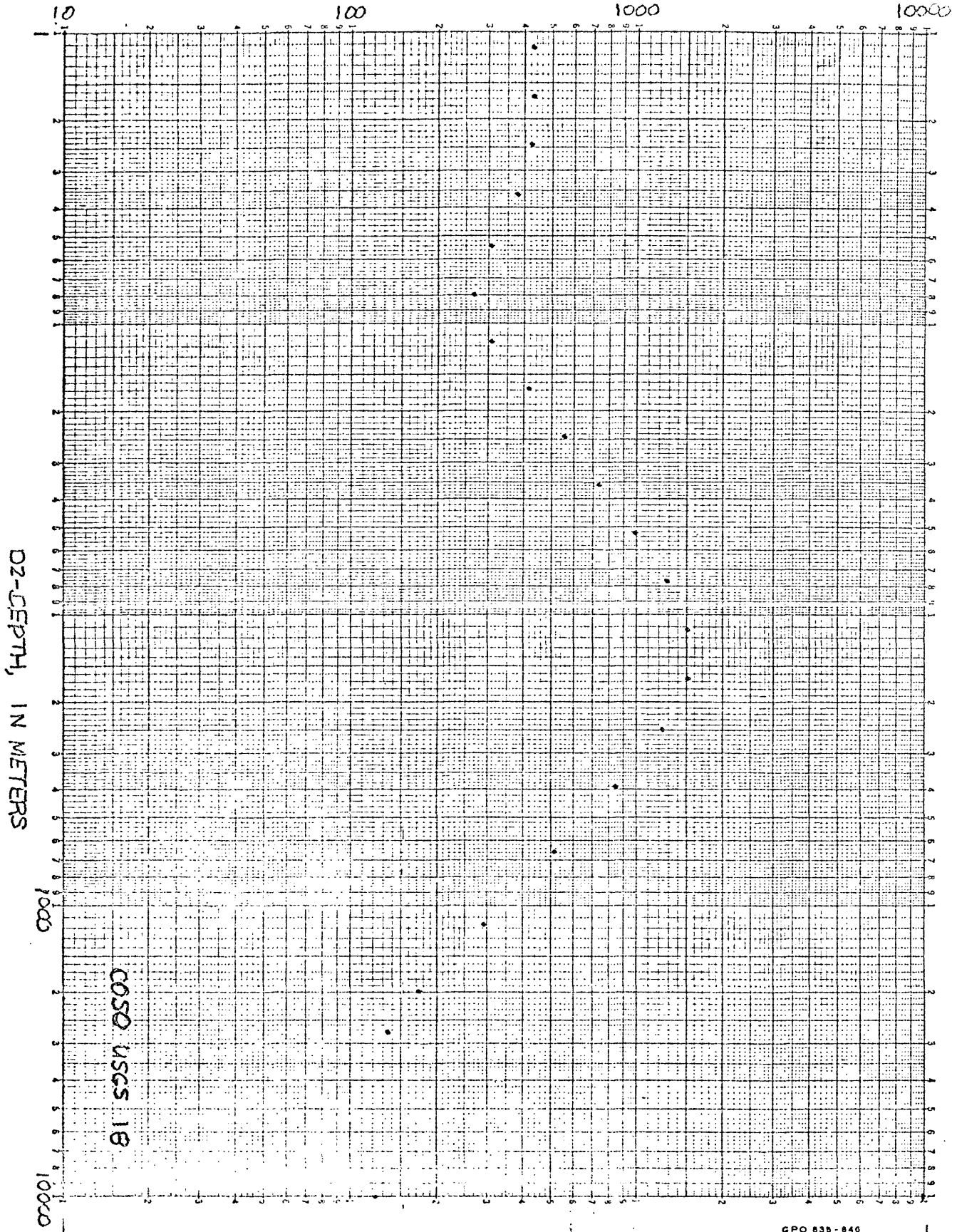
RESISTIVITIES IN OHM-METERS



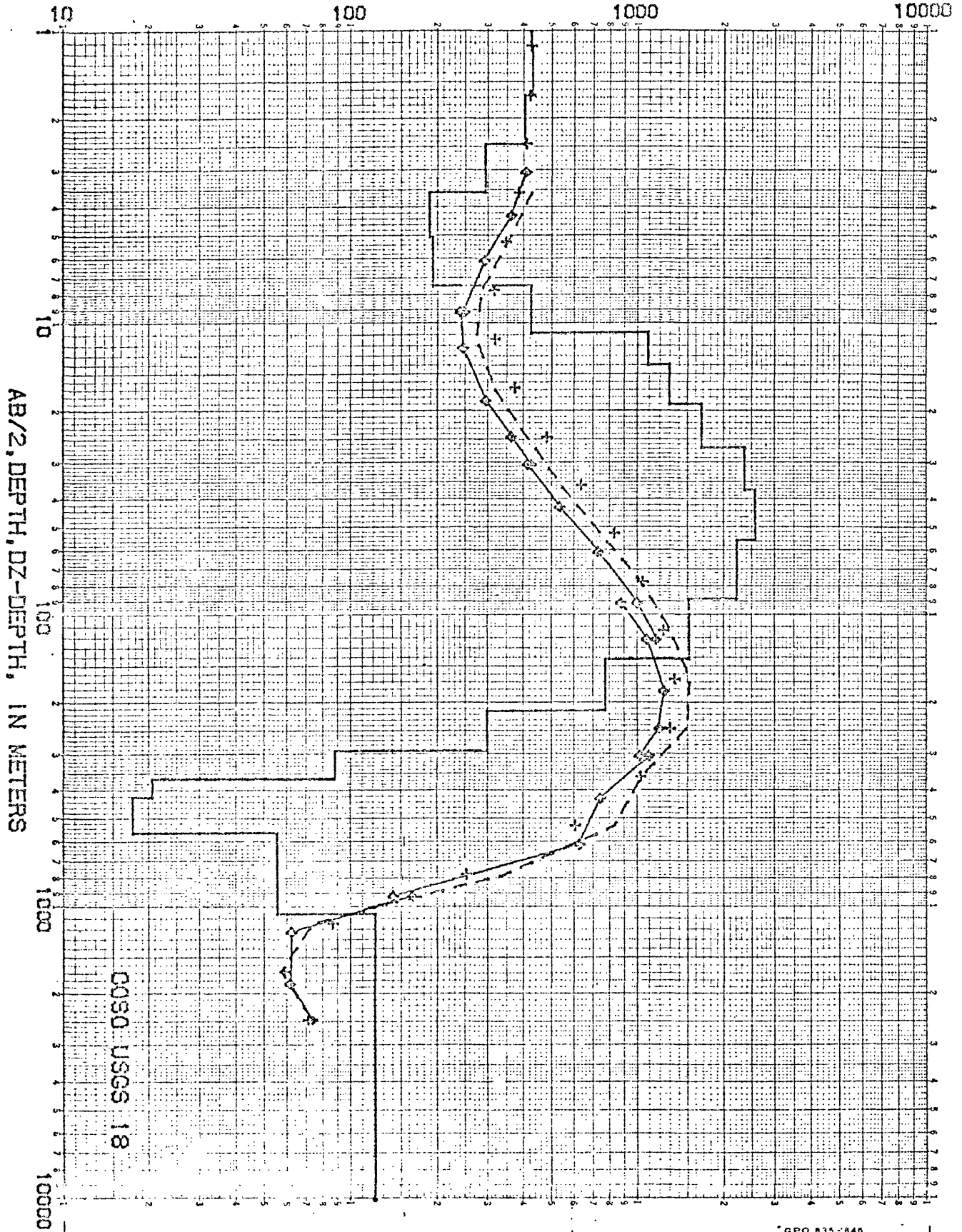
RESISTIVITIES IN OHM-METERS



RESISTIVITIES IN OHM-METERS

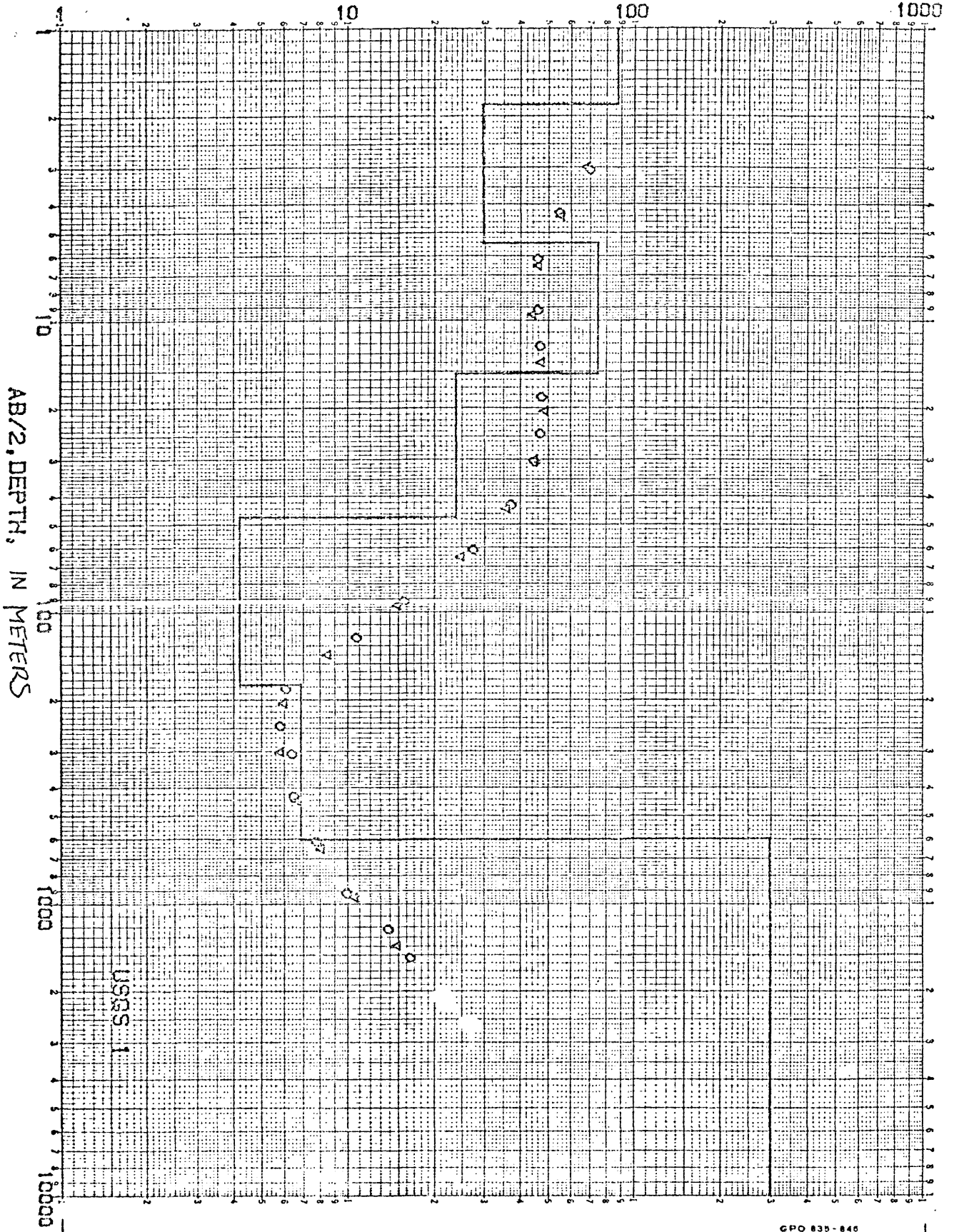


RESISTIVITIES IN OHM-METERS

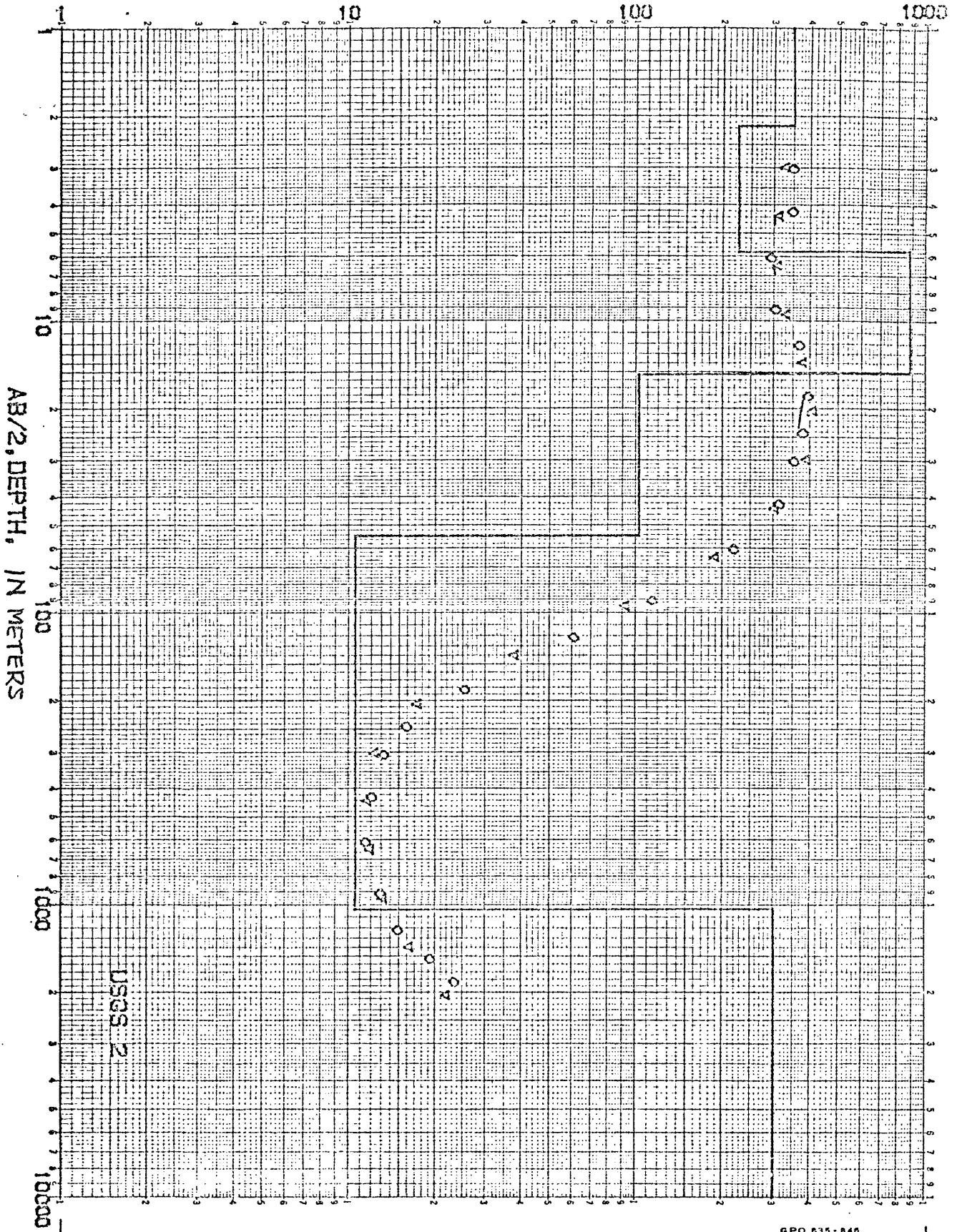


APPENDIX II

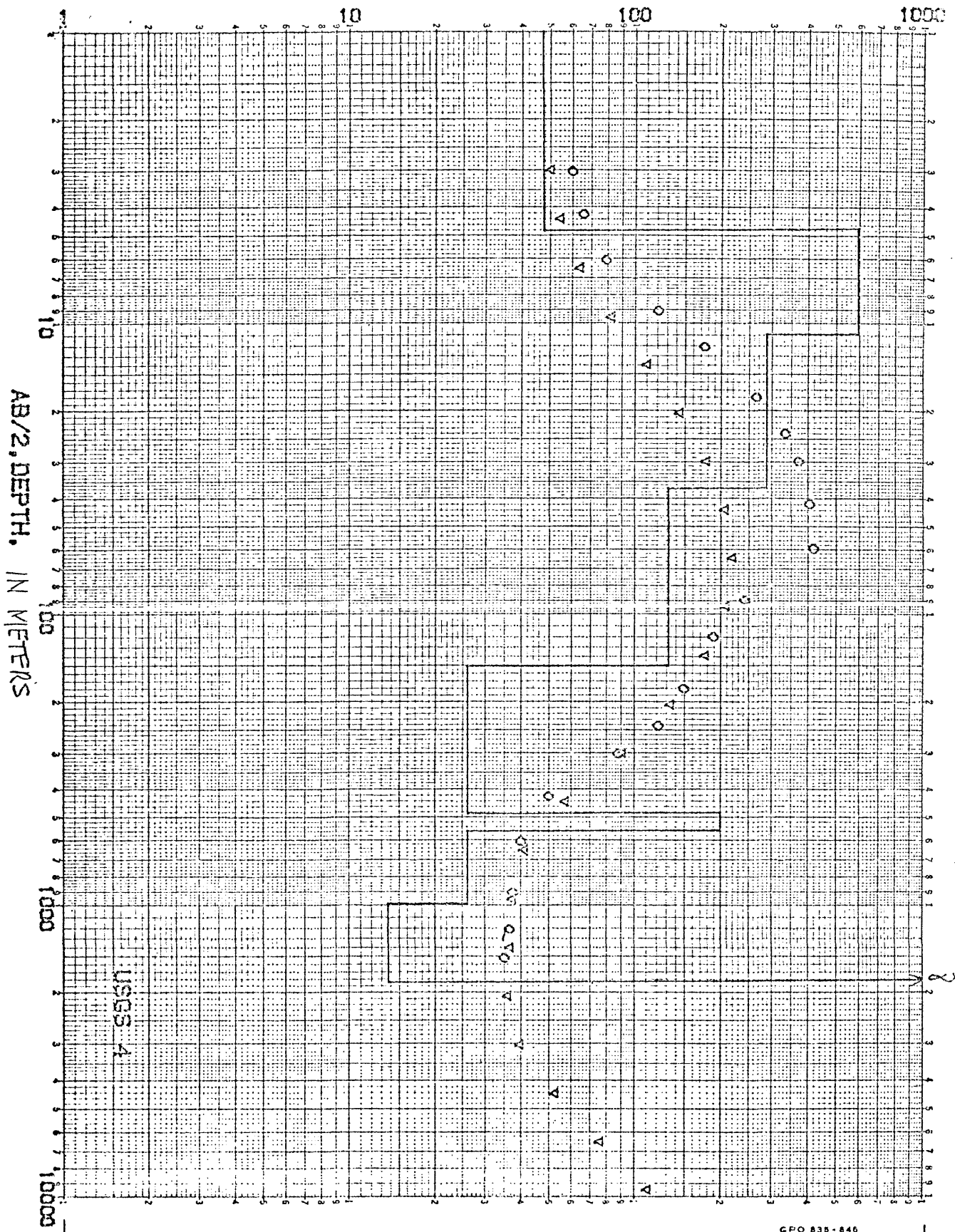
RESISTIVITIES IN OHM-METERS



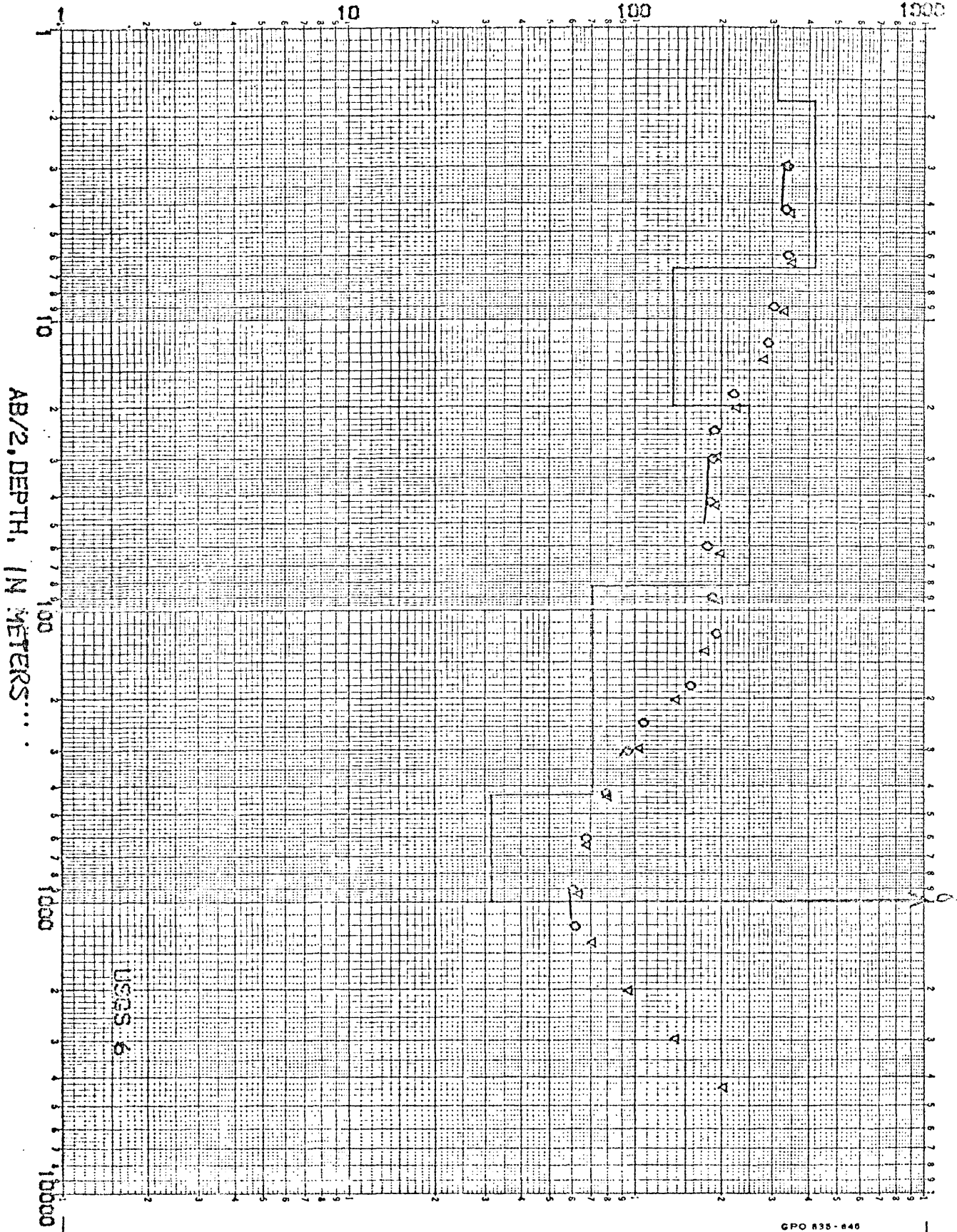
RESISTIVITIES IN OHM-METERS



RESISTIVITIES IN OHM-METERS

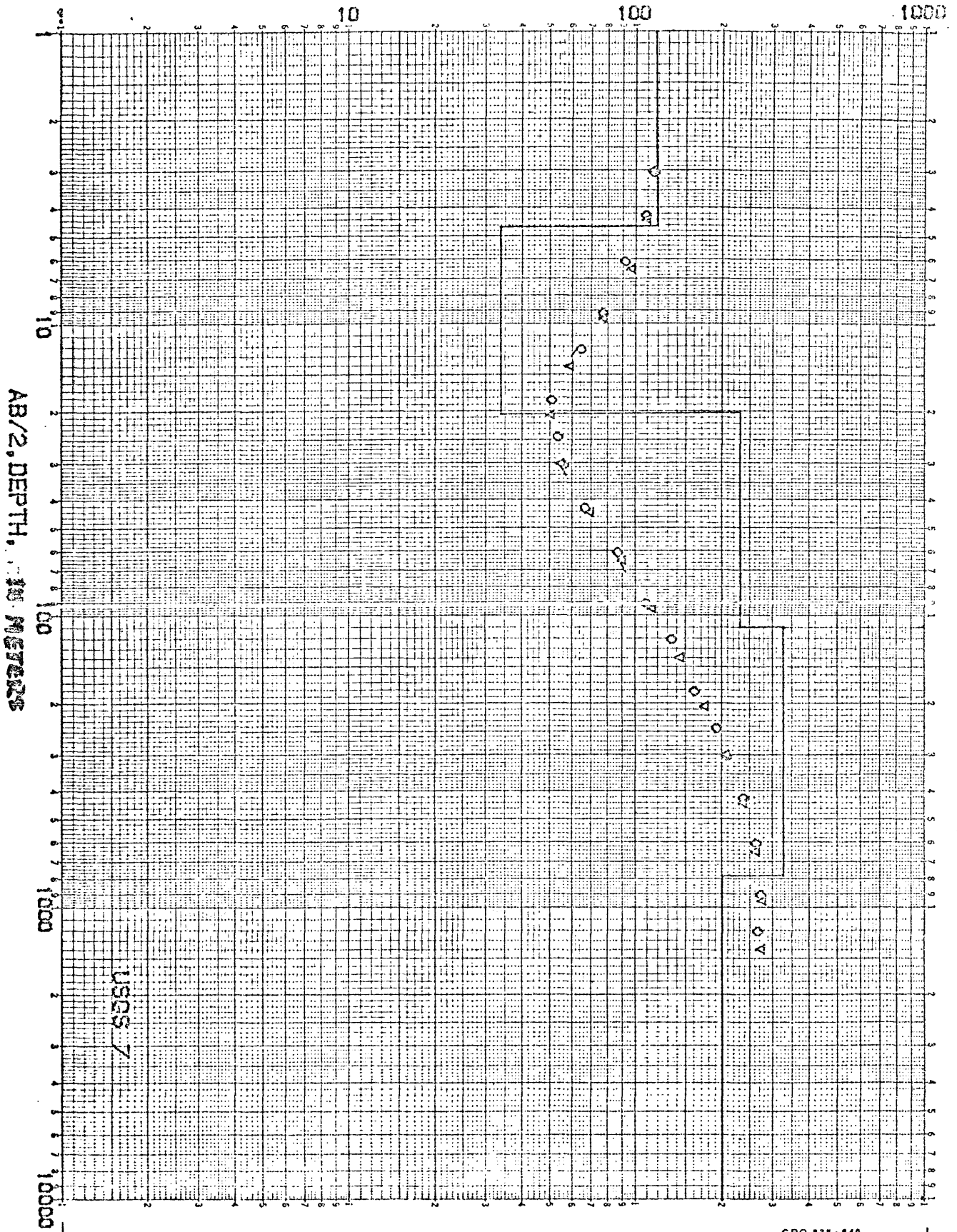


RESISTIVITIES IN OHM-METERS

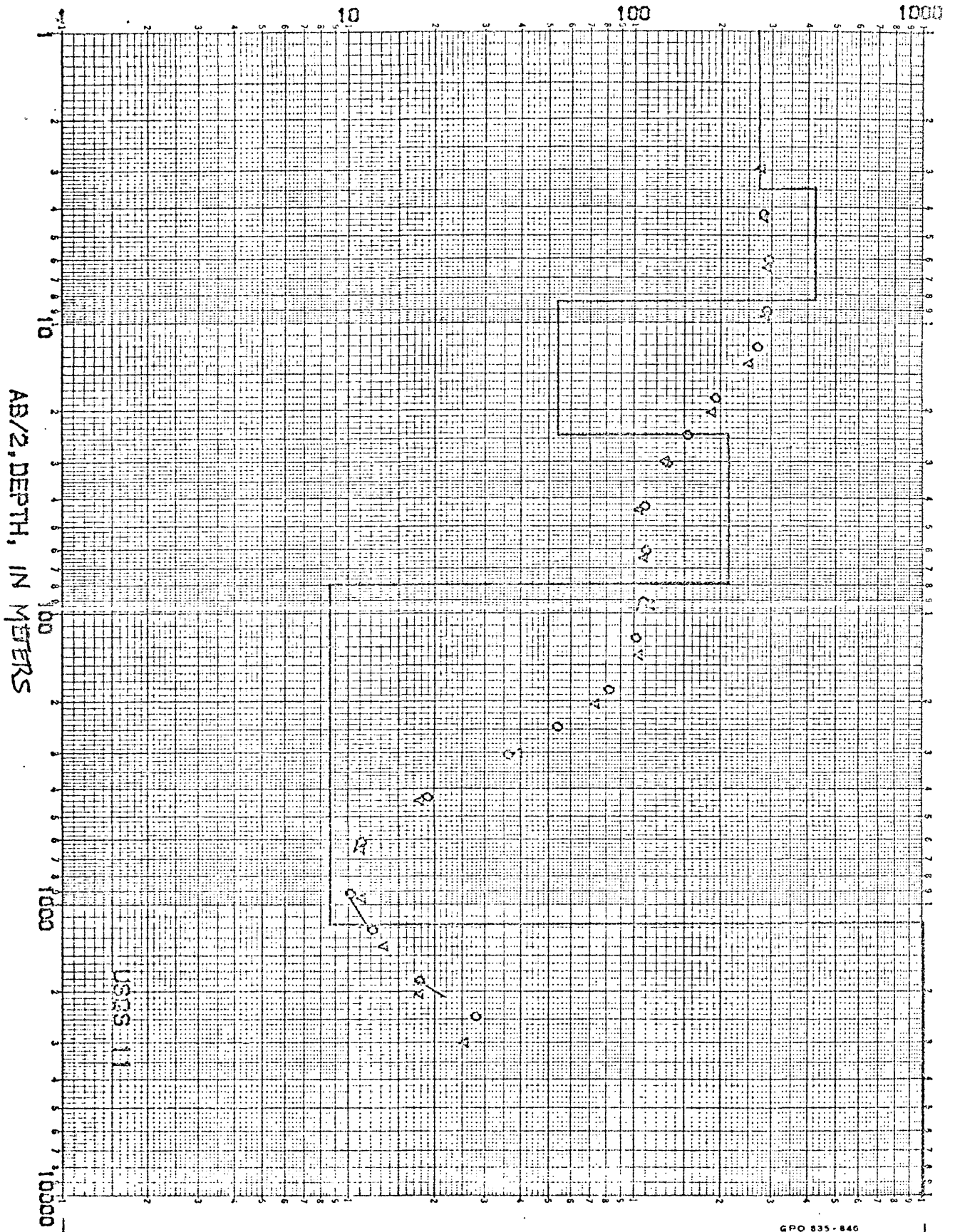


GPO 835-646

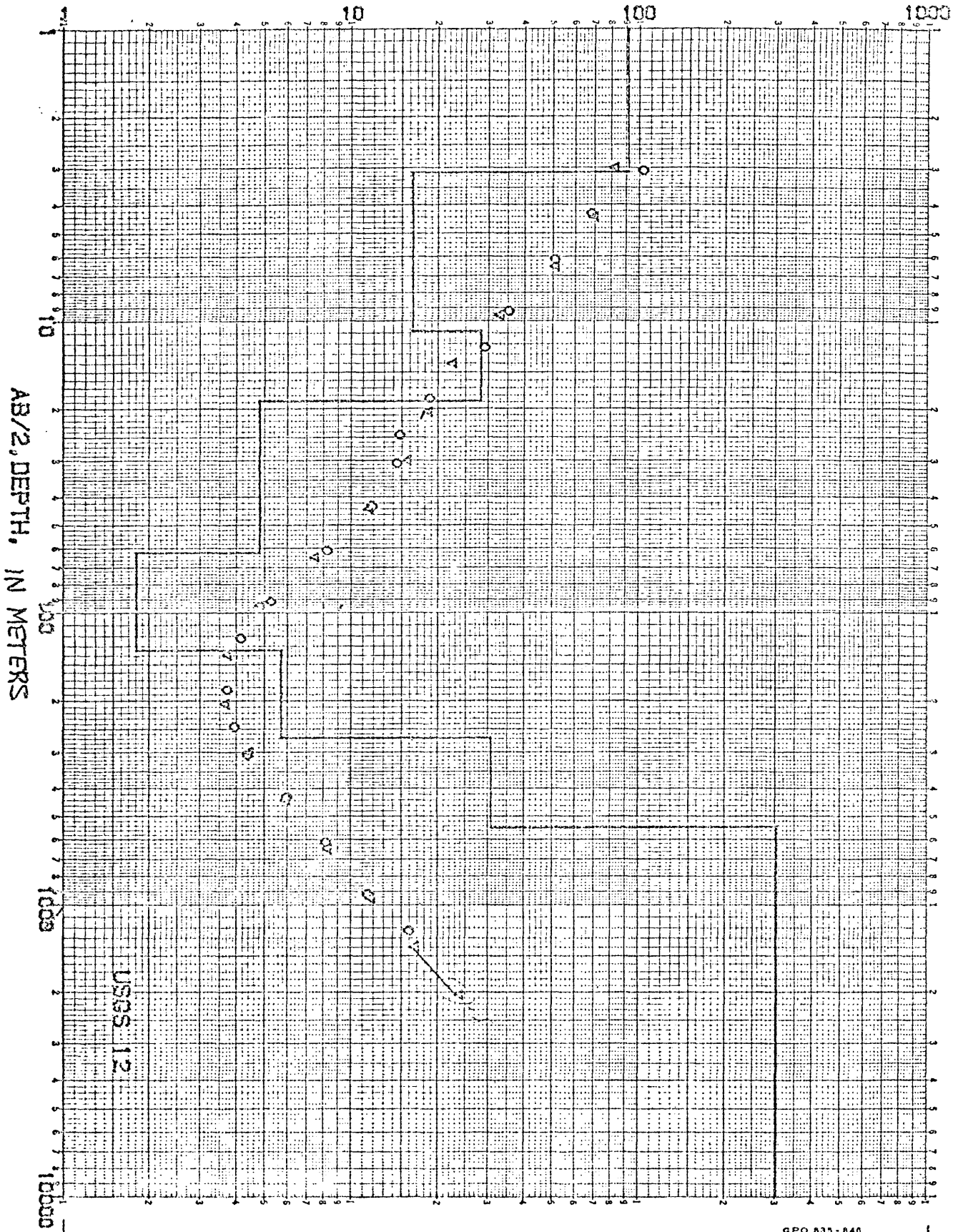
RESISTIVITIES IN OHM-METERS



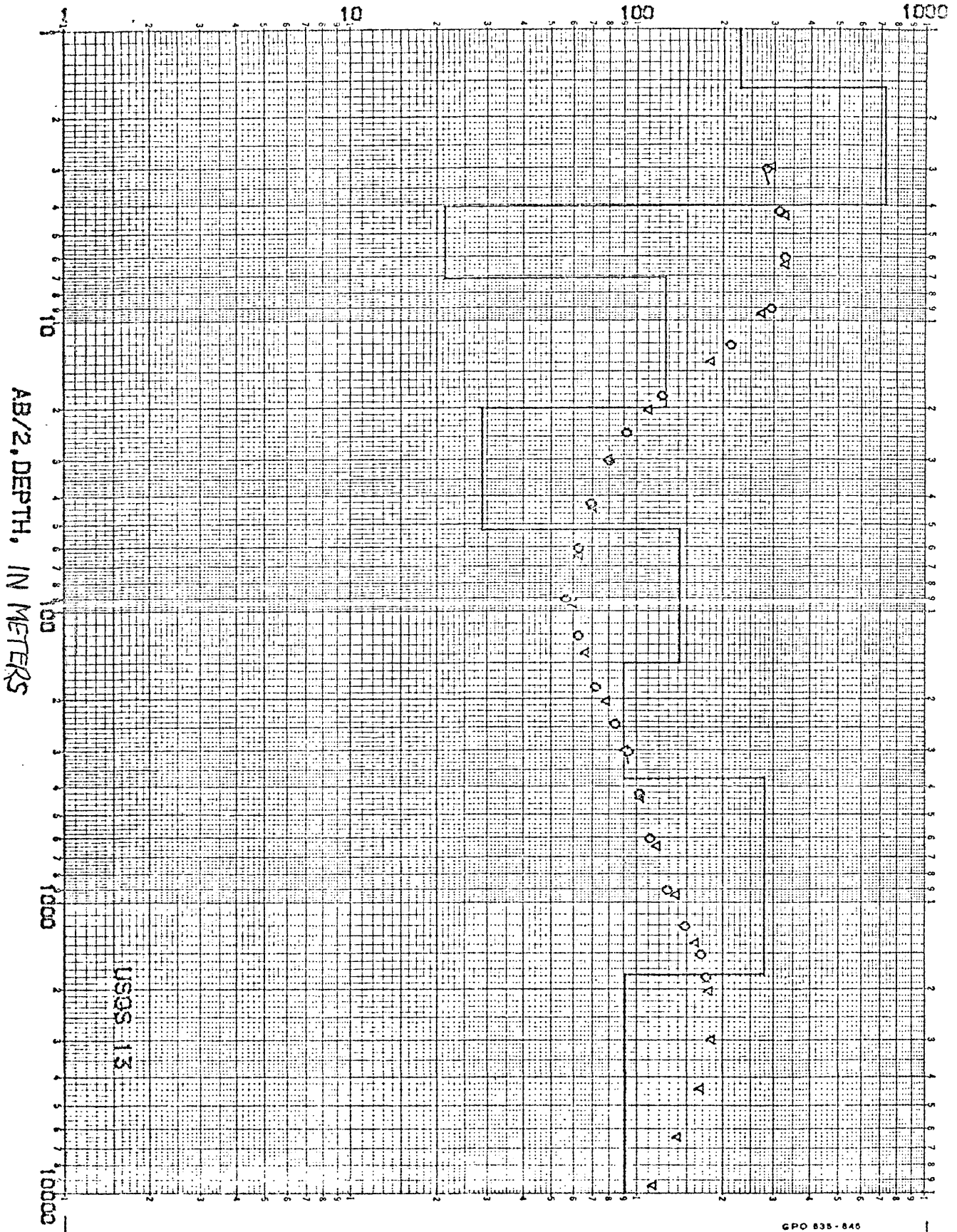
RESISTIVITIES IN OHM-METERS



RESISTIVITIES IN OHM-METERS

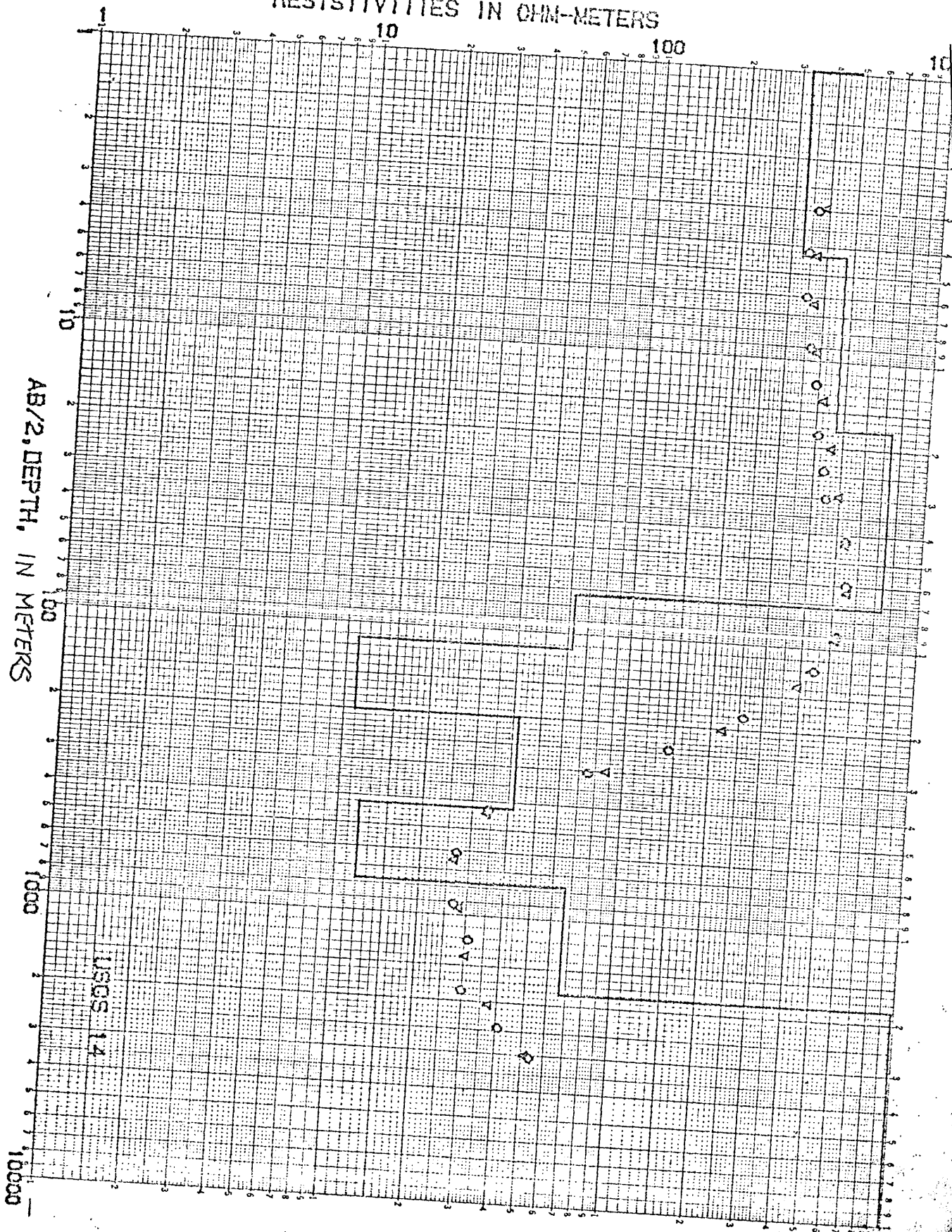


RESISTIVITIES IN OHM-METERS

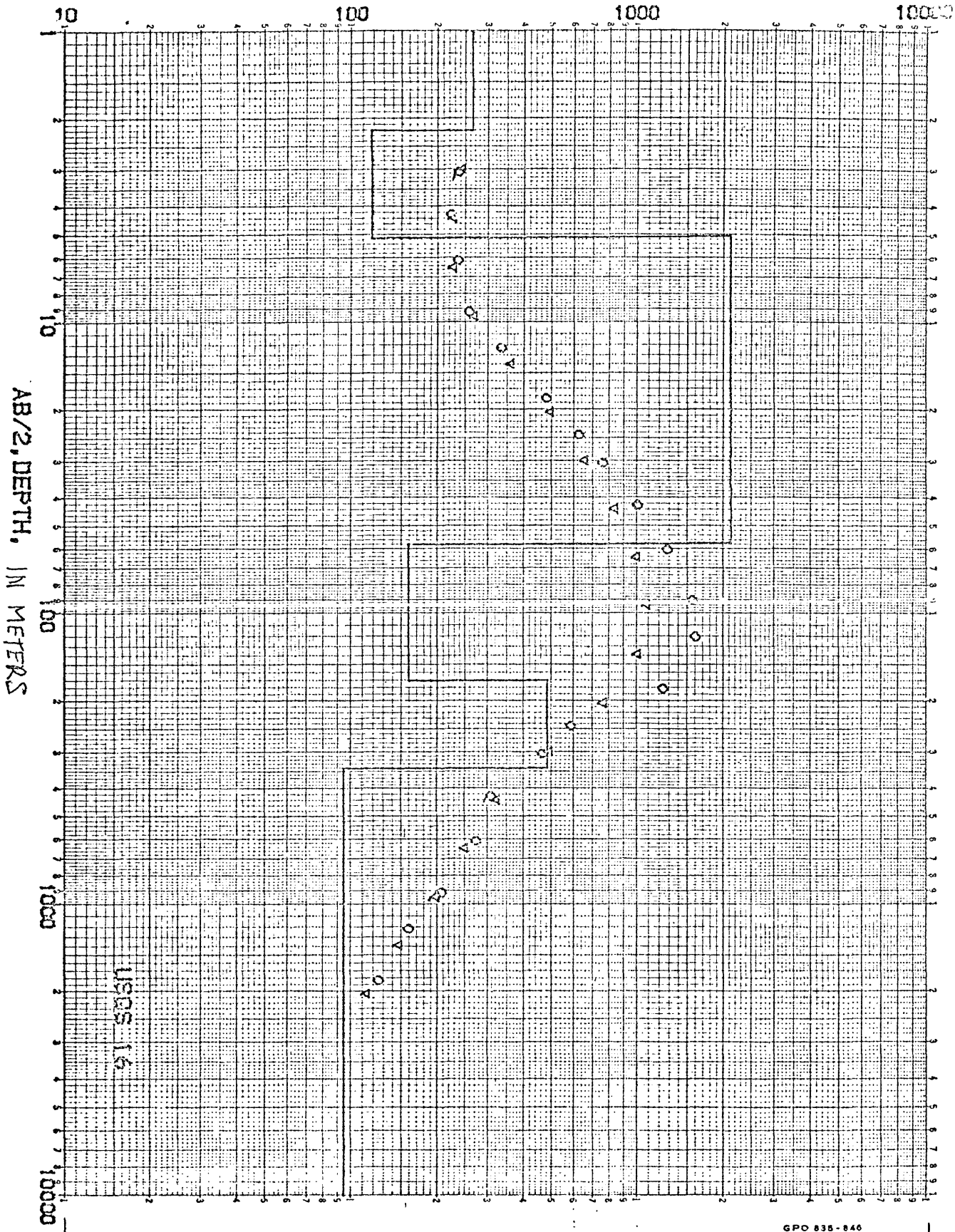


USGS 13

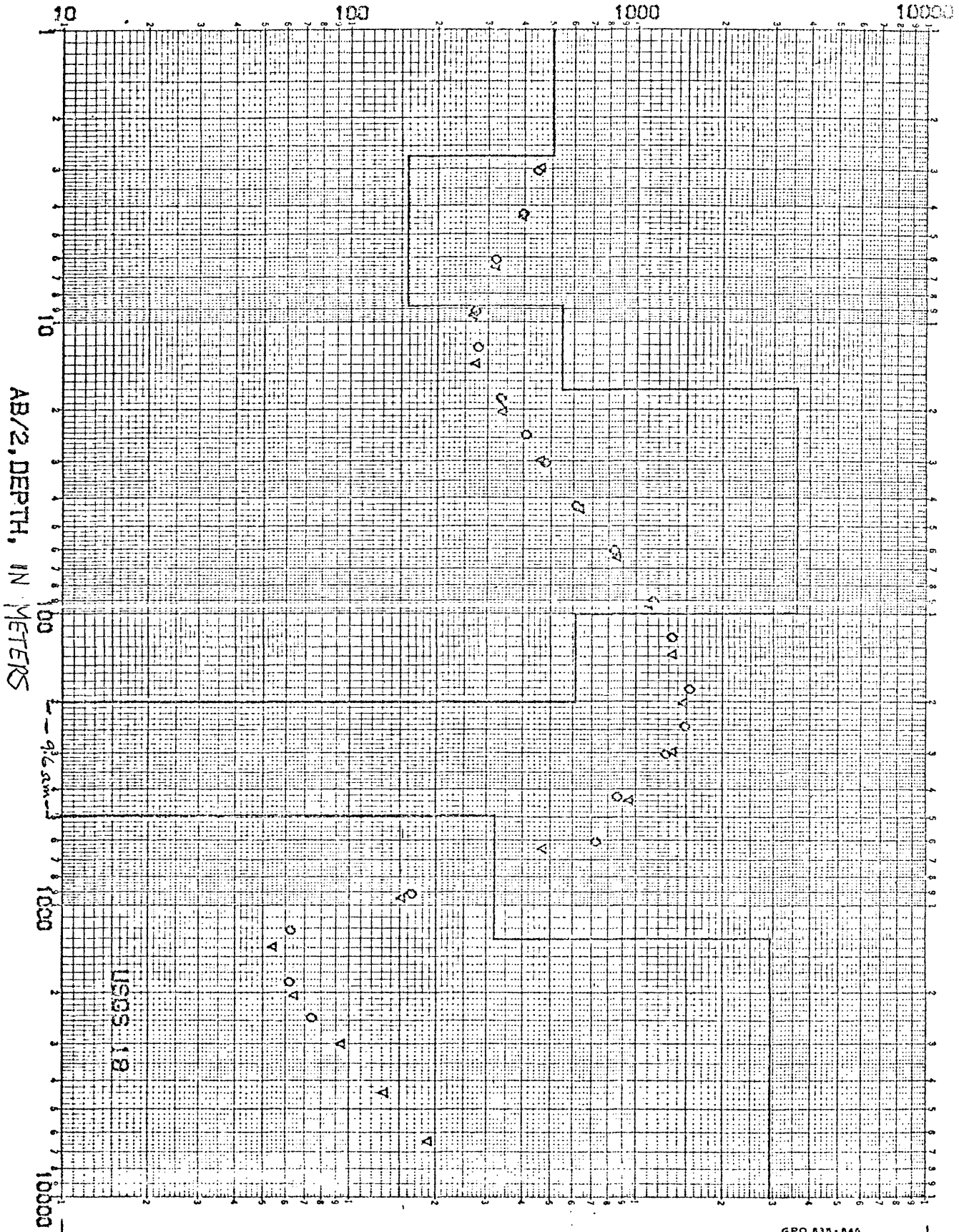
RESISTIVITIES IN OHM-METERS



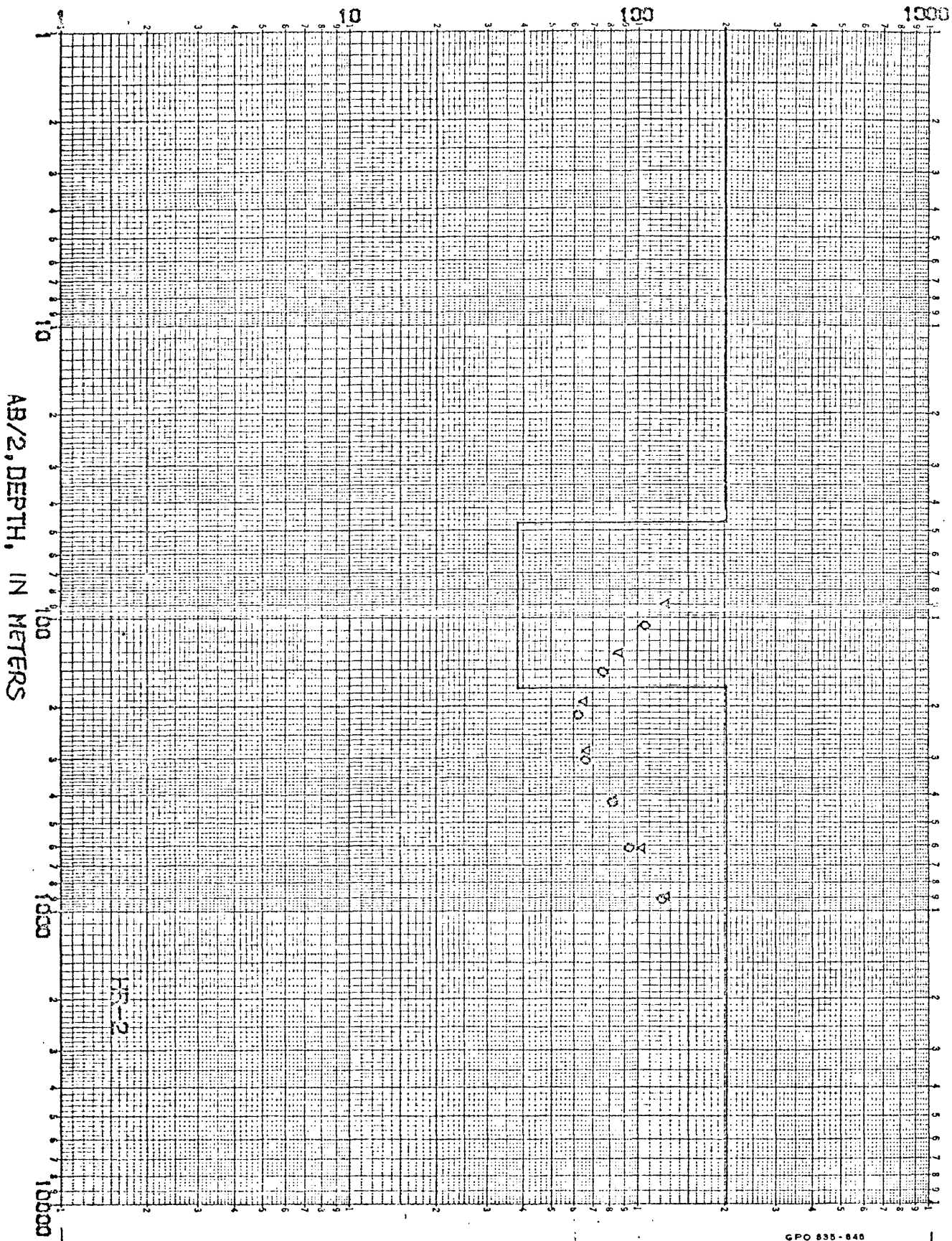
RESISTIVITIES IN OHM-METERS



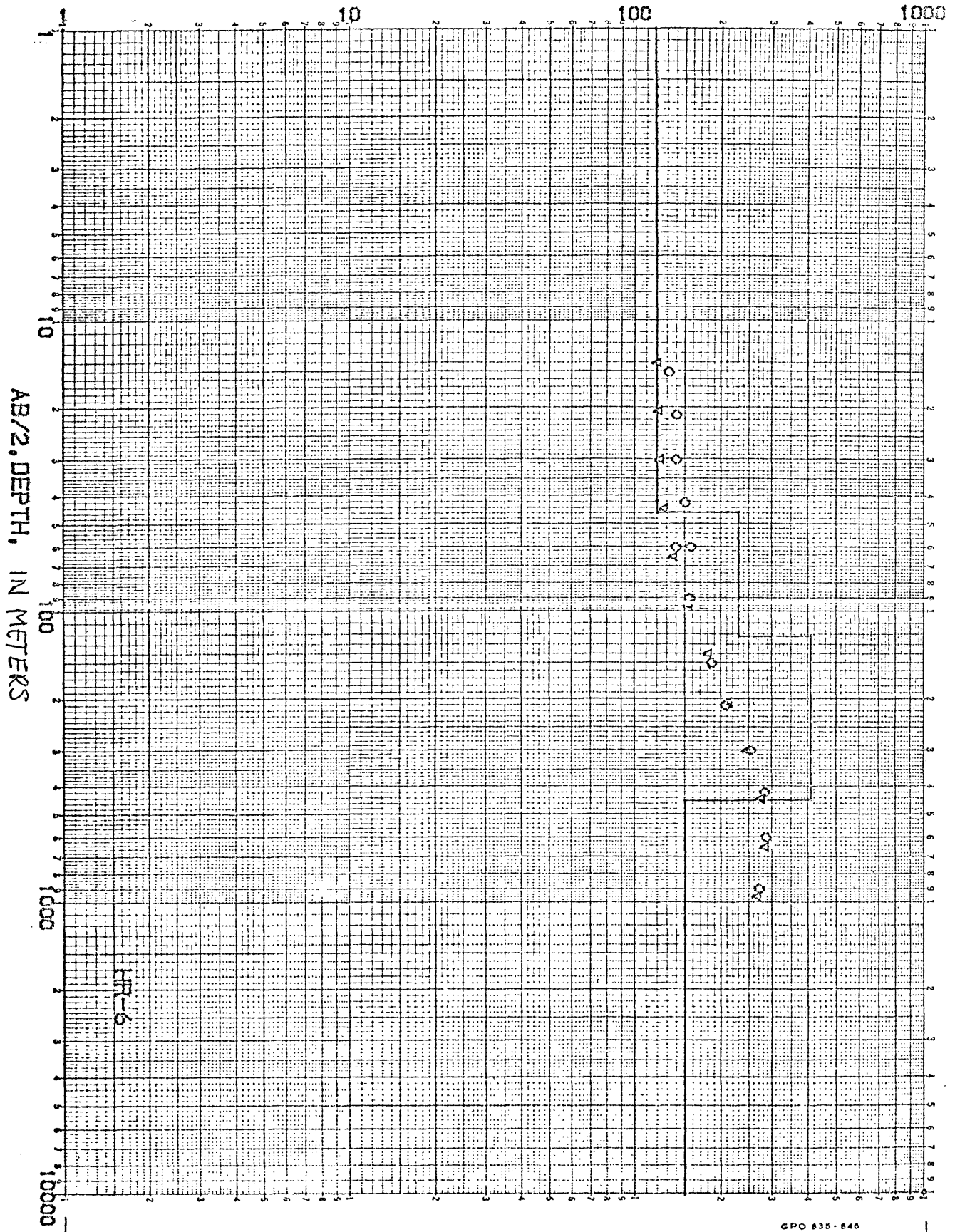
RESISTIVITIES IN OHM-METERS



RESISTIVITIES IN OHM-METERS

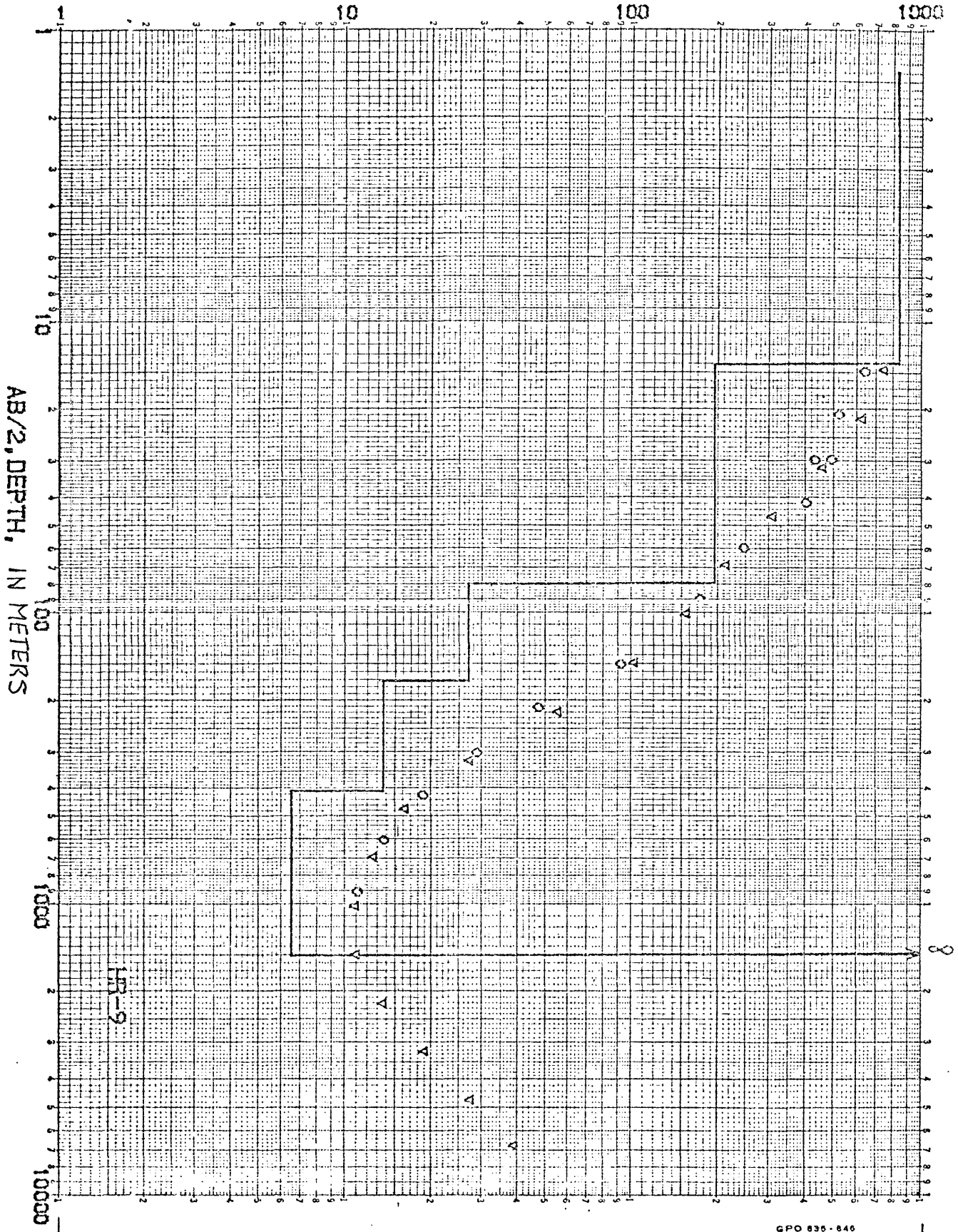


RESISTIVITIES IN OHM-METERS



GPO 835-840

RESISTIVITIES IN OHM-METERS



GPO 835-646

RESISTIVITIES IN OHM-METERS

